An introduction to black holes

Sanjeev S. Seahra

February 6, 2006

Contents

1 The Schwarzschild Geometry

1.1 The metric

Suppose that we are confronted with the following physical situation: we have some body floating about in outer space very far away from anything. This body is perfectly spherical, and in our frame of reference it is non-rotating. Furthermore, it is utterly static and we assume that it has always been that way, and will continue to be that way forever. Our job is to solve the Einstein field equations outside the body for the metric $g_{\alpha\beta}$ describing the curvature of spacetime induced by its presence. Since there is no matter in the exterior region, we know the field equations there will be

$$G_{\alpha\beta} = 0. \tag{1}$$

A direct attack on these equations is difficult, so let us first use the symmetries of the problem to make a reasonable guess as to what our final solution might look like. Our logic runs as follows:

1. At some instant of time, we draw a series of 2-dimensional spheres (2-spheres) concentric around the body. For each sphere, we measure its surface area and *define* its radius by $r = \text{area}/4\pi^2$. Then, we choose coordinates on each of the spheres such that the metric on the sphere of radius r is

$$ds^2_{(r,t)} = r^2(d\theta^2 + \sin^2\theta\, d\phi^2) = r^2\, d\Omega^2, \tag{2}$$

   where θ and ϕ are the usual spherical angles. The subscript on ds^2 stresses that each sphere is a surface of constant radius and time.

2. In principle, the angular coordinates on each of our spheres can be selected independently of each other; i.e., the north poles on adjacent spheres need not point in the same direction, or the half-circles defined by $(t, r, \phi) =$ constant need not lie in the same plane. This is not the most convenient choice, so let us demand that north poles are parallel and that the $(t, \phi) =$ constant surface defines a half-plane; in other words, we demand that the lines $(t, \theta, \phi) =$ constant run normal to the surface of the 2-spheres. Hence the metric on a constant time slice of our 4-manifold is

$$ds^2_{(t)} = h\, dr^2 + r^2\, d\Omega^2, \tag{3}$$

   where h is an unknown metric function. Because we have set $g_{r\theta} = g_{r\phi} = 0$, we are guaranteed that a vector in the r direction is orthogonal to the surface of the 2-spheres. What is the functional dependence of h? Well, our system is independent of time, so it is safe to assume that h is as well. Also, the spherical symmetry rules out any dependence on the angular coordinates. Hence, we conclude $h = h(r)$.

3. Now, the full metric is obtained by linking our spatial segments together. The most general way to do this is

$$ds^2 = -f\, dt^2 + h\, dr^2 + r^2\, d\Omega^2 + \mathbf{A}\cdot\mathbf{dx}\, dt, \tag{4}$$

   where

$$\mathbf{A}\cdot\mathbf{dx} = A_r\, dr + A_\theta\, d\theta + A_\phi\, d\phi. \tag{5}$$

We have introduced four new metric functions f and $\mathbf{A}$, which can all be considered to be functions of r only due to time invariance. But notice that when we make the substitution $t \to -t$, the metric becomes

$$ds^2 = -f\,dt^2 + h\,dr^2 + r^2\,d\Omega^2 - \mathbf{A}\cdot\mathbf{dx}\,dt, \tag{6}$$

which is not the same as (4). But our system ought to be insensitive to direction that time runs; i.e., it is entirely time reversible.[1] So this leads us to conclude that $\mathbf{A} = 0$ by time reversal invariance. So we come to the metric *ansatz* for the spacetime around our body:

$$ds^2 = -f\,dt^2 + h\,dr^2 + r^2\,d\Omega^2. \tag{7}$$

In the course of deriving this *ansatz* we have made use of several characteristics of our spacetime that have special names:

- a spacetime is said to be *stationary* if one can find a coordinate system in which its metric is independent of time
- a spacetime is *static* if it is stationary and its metric is invariant under time reversal in some set of coordinates
- a spacetime is *spherically symmetric* if a coordinate system can be found where the spatial part of the metric is invariant under the set of 3-dimensional rotations

These are actually fairly crude definitions of these terms, but we will refine them in the next section. Equation (7) represents the general line element for static and spherically symmetric spacetimes.

Now, we can use (7) to actually solve the field equations. Using GRTensor, we find that

$$G^t{}_t = -\frac{h'r + h(h-1)}{r^2h^2}, \quad G^r{}_r = -\frac{-f'r + f(h-1)}{hfr^2}, \tag{8}$$

where a prime indicates d/dr. By setting these equal to zero, we have a very simple system of ODEs to solve. The answer is:

$$f = C_2\left(1 - \frac{C_1}{r}\right), \quad h = \left(1 - \frac{C_1}{r}\right)^{-1}, \tag{9}$$

where C_1 and C_2 are integration constants. But if we re-scale our time coordinate according to $t \to t/\sqrt{C_2}$, we can essentially remove one of the constants from the problem. So our final solution is

$$ds^2 = -f\,dt^2 + \frac{1}{f}\,dr^2 + r^2\,d\Omega^2, \quad f = 1 - \frac{C}{r}, \tag{10}$$

where C is our only integration constant. This is the Schwarzschild metric. But hold on, what about the other components of the Einstein tensor? That is, we have found a solution to $G^t{}_t = G^r{}_r = 0$, but does this ensure that all of the components of $G_{\alpha\beta}$ equal zero? It turns out that the answer is yes, but this has to be checked explicitly.

[1] This would not be the case for a rotating system, because time reversal would flip the direction of the total angular momentum.

1.2 Killing vectors and symmetries

Before continuing with our investigation of the Schwarzschild solution, it is useful to introduce the concept of a Killing vector. They will be very useful for the upcoming calculations.

A vector ξ^α is a Killing vector if it satisfies Killing's equation:

$$0 = \nabla_\alpha \xi_\beta + \nabla_\beta \xi_\alpha, \tag{11}$$

or in other words, $\nabla_\alpha \xi_\beta$ is an anti-symmetric tensor. One of the primary uses of Killing vectors is to find constants of the motion for particles following geodesics. To see how this works, consider some geodesic trajectory with 4-velocity $u^\alpha = dx^\alpha/d\tau = \dot{x}^\alpha$ where τ is the proper time such that $u^\alpha u_\alpha = -1$.[2] Now consider

$$\begin{aligned} u^\alpha \nabla_\alpha u^\beta &= u^\alpha(\partial_\alpha u^\beta + \Gamma^\beta_{\alpha\gamma} u^\gamma) \\ &= \frac{dx^\alpha}{d\tau}\frac{\partial}{\partial x^\alpha}\frac{dx^\beta}{d\tau} + \Gamma^\beta_{\alpha\gamma}\frac{dx^\alpha}{d\tau}\frac{dx^\gamma}{d\tau} \\ &= \frac{d^2x^\beta}{d\tau^2} + \Gamma^\beta_{\alpha\gamma}\frac{dx^\alpha}{d\tau}\frac{dx^\gamma}{d\tau} \\ &= 0, \end{aligned} \tag{12}$$

where the last step follows from the geodesic equation. Hence, we see that $u^\alpha \nabla_\alpha u^\beta = 0$ is in some sense equivalent to the geodesic equation. In general, $v^\alpha \nabla_\alpha v^\beta$ is *defined* to be the 4-acceleration of an arbitrary vector field v^α; hence, the geodesic equation merely states that the covariant acceleration of a particle's 4-velocity is zero.

Now consider the scalar product of the 4-velocity of a geodesic path with a Killing vector. In particular, what is the proper time derivative of this quantity?

$$\begin{aligned} \frac{d}{d\tau}(u^\alpha \xi_\alpha) &= \frac{dx^\beta}{d\tau}\frac{\partial}{\partial x^\beta}(u^\alpha \xi_\alpha) \\ &= \frac{dx^\beta}{d\tau}\nabla_\beta(u^\alpha \xi_\alpha) \\ &= u^\beta(u^\alpha \nabla_\beta \xi_\alpha + \xi_\alpha \nabla_\beta u^\alpha) \\ &= \tfrac{1}{2} u^\alpha u^\beta(\nabla_\alpha \xi_\beta + \nabla_\beta \xi_\alpha) \\ &= 0. \end{aligned} \tag{13}$$

In going from the second to the third line we used $u^\alpha \nabla_\alpha u^\beta = 0$, and from the third to fourth line we used the Killing equation. Hence $u^\alpha \xi_\alpha$ is conserved along the trajectory.

Killing vectors are also intimately related to the symmetries of the spacetime. For example, consider a situation where a metric is independent of a certain coordinate in a certain coordinate system, say q. Then, we claim that $\xi^\alpha = \partial/\partial q$ is a Killing vector on that spacetime.[3] To see this, let us assume $\xi^\alpha = \partial_q$ and consider

$$\begin{aligned} \nabla_\alpha \xi^\beta + \nabla^\beta \xi_\alpha &= \nabla_\alpha \xi^\beta + g^{\beta\mu} g_{\alpha\nu} \nabla_\mu \xi^\nu \\ &= \Gamma^\beta_{\alpha\lambda}\xi^\lambda + g^{\beta\mu} g_{\alpha\nu}\Gamma^\nu_{\mu\lambda}\xi^\lambda \\ &= \tfrac{1}{2} g^{\beta\gamma}(\partial_\alpha g_{\lambda\gamma} + \partial_\lambda g_{\alpha\gamma} - \partial_\gamma g_{\alpha\lambda} + \partial_\gamma g_{\lambda\alpha} + \partial_\lambda g_{\gamma\alpha} - \partial_\alpha g_{\gamma\lambda})\xi^\lambda. \end{aligned}$$

[2] We will always use an overdot to indicate differentiation with respect to proper time (or affine parameter for null paths).

[3] Just a word about our notation for vectors: we often will write things like $v^\alpha = v^x \partial_x + v^y \partial_y + \cdots$; in such formulae, the partial derivative operators act as place holders. That is, the coefficient of ∂_x is the x-component of the v^α vector, etc... In a similar vein, we write one-forms as $v_\alpha = v_x dx + v_y dy + \cdots$

In going from the first to the second line we made use of $\partial_\alpha \xi^\beta = 0$ (which is only true in our special coordinate system) and to go from the second to the third we used $\partial_\alpha \delta^\beta_\gamma = 0$ as well as the standard definitions of the Christoffel symbols. Simplifying the above, we obtain

$$\nabla_\alpha \xi_\beta + \nabla_\beta \xi_\alpha = \xi^\lambda \partial_\lambda g_{\alpha\beta} = \frac{\partial}{\partial q} g_{\alpha\beta}. \tag{14}$$

Therefore, if the metric is independent of q, $\xi^\alpha = \partial_q$ is a Killing vector on the spacetime manifold. The argument can also be run in the reverse direction: if ξ^α is a Killing vector and we can find a coordinate system in which $\xi^\alpha = \partial_q$ (which is always possible), then the metric will be independent of q in that system.

Getting back to the Schwarzschild manifold, there are two obvious Killing vectors that reflect the independence of the metric on t and ϕ:

$$\xi^\alpha_{(t)} = \partial_t, \quad \xi^\alpha_{(\phi)} = \partial_\phi. \tag{15}$$

The first represents the time symmetry of the system, while the second reflects the invariance of the metric under rotations about the z-axis. Of course, the geometry ought to be invariant under rotations about the x and y axes, so there are two other Killing vectors:

$$\xi^\alpha_{(1)} = \sin\phi\, \partial_\theta + \cot\theta \cos\phi\, \partial_\phi, \quad \xi^\alpha_{(2)} = -\cos\phi\, \partial_\theta + \cot\theta \sin\phi\, \partial_\phi. \tag{16}$$

The existence of these Killing vectors makes our previous definitions of stationarity, staticity, and spherical symmetry more concrete:

- a spacetime is *stationary* if it has a timelike Killing vector,
- a spacetime is *static* if that timelike Killing vector is orthogonal to the hypersurfaces of constant t,
- a spacetime is *spherically symmetric* if it has a set of Killing vectors corresponding to rotations about 3-orthogonal axes.[4]

1.3 Singularities and horizons

The properties of the metric function f have some significant implications for the Schwarzschild geometry. We have the following limits:

$$\lim_{r\to\infty} f = 1, \quad \lim_{r\to C} f = 0, \quad \lim_{r\to 0} f = -\infty. \tag{17}$$

The first of these implies that the geometry is asymptotically flat for large values of r. This is reassuring because it implies that gravitational field of the central body dies off at great distances. The middle limit is somewhat worrisome, because it implies that $g_{tt} = 0$ and $g_{rr} \to \pm\infty$, depending on the direction of approach. Clearly then, if our body has radius less than C then the exterior geometry will involve an $r =$ constant hypersurface across which the metric is discontinuous and non-finite. There is a similar problem at $r = 0$, where the g_{tt} component diverges while the g_{rr} component vanishes.

So what are we to make of these surfaces where the metric has pathological behaviour? We note that the "timelike" Killing vector $\xi^\alpha_{(t)}$ actually becomes null on the

[4]The last definition is still somewhat vague, but the proper explanation is beyond the scope of these lectures; however see Exercise 3 for a partial explanation.

$r = C$ surface. This means $r = C$ is a *Killing horizon*; i.e., a place where the signature of a Killing vector changes. Inside the horizon, which we denote by $\mathcal{H}$, $\xi^\alpha_{(t)}$ is actually spacelike. This means that t behaves like a spacelike coordinate and r behaves like a timelike coordinate inside of $\mathcal{H}$. We will see below that this has rather dire implications for anybody unlucky enough to find themselves within the Killing horizon.

It would seem that the Killing horizon is — in some sense — singular because the metric is badly behaved there. But in precisely what sense? For example, does the curvature of the manifold diverge on $\mathcal{H}$? To investigate, we can calculate the Kretschmann scalar for the Schwarzschild geometry:

$$R^{\alpha\beta\gamma\delta}R_{\alpha\beta\gamma\delta} = \frac{12C^2}{r^6}. \tag{18}$$

This is an invariant quantity; i.e., it takes the same value in all coordinate systems. Notice that it is manifestly finite on $\mathcal{H}$, but it blows up at $r = 0$. If we were to calculate all the other possible scalars formed from the curvature tensor $R_{\alpha\beta\gamma\delta}$, we would find that they are all finite along $\mathcal{H}$. So, $\mathcal{H}$ is certainly not a *curvature singularity*. But, it is the position of a *coordinate singularity*; i.e., a place where the metric is badly behaved in a certain coordinate system. However, the existence of a coordinate singularity in a given spacetime is not cause for front page news; such objects can be generated by poor choice coordinates on perfectly regular manifolds. For example, consider the 2-metric:

$$ds^2 = -x^2\,dt^2 + dx^2. \tag{19}$$

This metric has a coordinate singularity at $x = 0$. But if we transform coordinates according to

$$x = \sqrt{X^2 - T^2}, \quad t = \operatorname{arctanh}\frac{T}{X}, \tag{20}$$

this becomes

$$ds^2 = -dT^2 + dX^2; \tag{21}$$

i.e., flat Minkowski space! In this case, the coordinate singularity at $x = 0$ is completely meaningless because the underlying manifold is regular, in every possible sense of the word. We must acknowledge the possibility that the coordinate singularity $\mathcal{H}$ in the Schwarzschild metric might be of the same calibre — entirely harmless.

But the same cannot be said of the singularity at $r = 0$. There, the Kretschmann scalar does blow up and there can be no doubt that the manifold itself is special there. No coordinate transformation can change this fact — $r = 0$ is a place where the geometry itself is poorly defined. So we call $r = 0$ a curvature singularity.

1.4 Observers and trajectories in Schwarzschild

1.4.1 The potential and constants of the motion for free particles

The best way to learn about a spacetime is to track the movement of observers through it. So with that in mind, let us calculate the potential governing the movement of freely-falling test particles through our spacetime. For later convenience, we will treat the cases of timelike, spacelike, and null particles simultaneously. At some instant of time, we choose spherical coordinates such that our particle is in the $\theta = \pi/2$ plane with their velocity oriented such that $\dot\theta = 0$. Then, using the $\xi^\alpha_{(1)}$ and $\xi^\alpha_{(2)}$ Killing vectors we

find the following constants of the motion:

$$g_{\alpha\beta}\xi^{\alpha}_{(1)}u^{\beta} = r^2(\dot{\theta}\sin\phi + \dot{\phi}\cos\theta\cos\phi) = 0, \tag{22a}$$

$$g_{\alpha\beta}\xi^{\alpha}_{(2)}u^{\beta} = r^2(-\dot{\theta}\cos\phi + \dot{\phi}\cos\theta\sin\phi) = 0. \tag{22b}$$

Together these imply that $\dot{\theta}^2 = \dot{\phi}^2\cos^2\theta$; which consistently implies that if $\theta = \pi/2$ initially, the particle will not leave the equatorial plane. Hence when studying geodesic motion, we can safely set $\theta = \pi/2$ and $\dot{\theta} = 0$.

Now there are two other Killing vectors that give rise to two more constants of the motion:

$$E = -g_{\alpha\beta}\xi^{\alpha}_{(t)}u^{\beta} = f\dot{t}, \quad L = g_{\alpha\beta}\xi^{\alpha}_{(\phi)}u^{\beta} = r^2\dot{\phi}. \tag{23}$$

Of these, L is readily recognized as the angular momentum (per unit mass) of our particle about the z-axis. Our notation for the other constant suggests that it is the energy, but let us defer that identification briefly.

These constants of the motion can now be used to simplify the 4-velocity normalization condition $u^{\alpha}u_{\alpha} = -\kappa$, where $\kappa = \pm 1, 0$ for timelike, spacelike, or null particles, respectively. We get:

$$-\kappa = -f\dot{t}^2 + \frac{1}{f}\dot{r}^2 + r^2\dot{\phi}^2 = \frac{\dot{r}^2 - E^2}{f} + \frac{L^2}{r^2}, \tag{24}$$

where we have made use of $\dot{\theta} = \sin\theta = 0$. This can be rearranged to get

$$\frac{1}{2}E^2 = \frac{1}{2}\dot{r}^2 + \frac{1}{2}\left(1 - \frac{C}{r}\right)\left(\frac{L^2}{r^2} + \kappa\right). \tag{25}$$

This looks suspiciously like a Newtonian conservation of energy equation. For a moment, consider the case of the purely radial motion ($L = 0$) of a timelike trajectory ($\kappa = +1$). Then we have

$$\frac{1}{2}(E^2 - 1) = \frac{1}{2}\dot{r}^2 - \frac{C}{2r}. \tag{26}$$

This is *exactly* the Newtonian expression of conservation of energy if we set $C = 2M$ (where M is the mass of the central body) and we identify $\frac{1}{2}(E^2 - 1)$ as the classical mechanical energy $E_{\text{classical}}$ of the particle, per unit mass. The latter is possible if we identify E as the total relativistic energy per unit rest mass of the particle (i.e., $E = 1 + E_{\text{classical}}$) and we work in the low energy regime $E_{\text{classical}} \ll 1$. So we have run down the meaning of the integration constant in our solution and found:

$$f = 1 - \frac{2M}{r}. \tag{27}$$

Furthermore, we have identified E as the total relativistic energy of our test particle, per unit mass.

1.4.2 Freely-falling massive observers

Let us now let L be non-zero but maintain $\kappa = +1$, so that we are considering general trajectories of massive test particles. The problem is essentially that of the one-dimensional motion of a particle with total energy $\frac{1}{2}E^2 > 0$ through the potential

$$V = \frac{1}{2}\left(1 - \frac{2M}{r}\right)\left(\frac{L^2}{r^2} + 1\right) \tag{28}$$

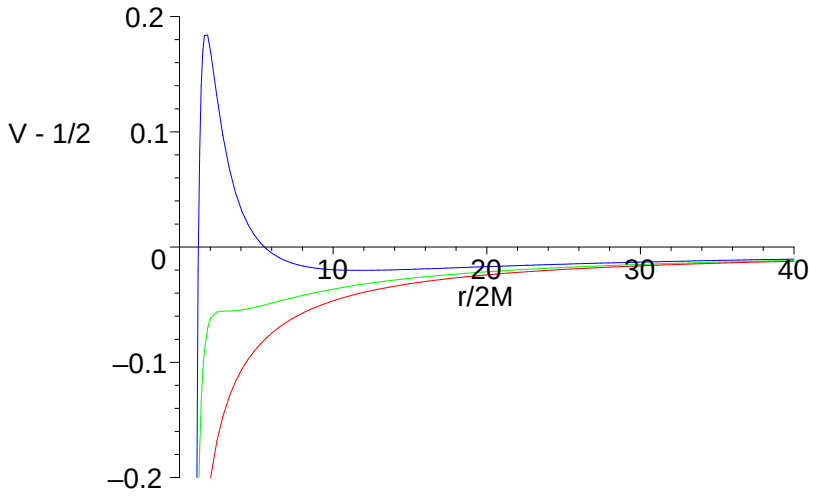

Figure 1: The potential governing the motion of massive test particles in the Schwarzschild geometry. From bottom to top, the curves correspond to $L/2M = \frac{1}{2}\sqrt{3}, \sqrt{3}, \frac{3}{2}\sqrt{3}$.

We plot this potential in Figure 1 for several different values of the ratio L/M. There are three types of curve are evident: one with a local maximum and minimum, one with an inflection point, and another with no local extrema. This implies that there may or may not be r-equilibrium positions — which represent circular orbits — depending on the value of the angular momentum.

To make this qualitative observation more robust, we can solve for the positions of the local extrema of V:

$$0 = \left.\frac{\partial V}{\partial r}\right|_{r=r_\pm} \quad \Rightarrow \quad r_\pm = \frac{L^2}{2M}\left(1 \pm \sqrt{1 - \frac{12M^2}{L^2}}\right). \tag{29}$$

Hence, there can be no equilibrium r positions if $L/2M < \sqrt{3}$. It is easy to verify that

$$\left.\frac{\partial^2 V}{\partial r^2}\right|_{r=r_+} = \frac{16M^4\sqrt{1 - 12M^2/L^2}}{L^6(1 + \sqrt{1 - 12M^2/L^2})^4} > 0, \tag{30}$$

so we know that r_+ is always a minimum of V. We also see that r_+ is always greater than $6M$, so stable circular test particle orbits can only occur at $r > 6M$. This gives rise to the terminology "innermost stable circular orbit (ISCO)" for the $r = 6M$ path. Similarly, one can show that $r = r_-$ always represents an unstable circular orbit.

It is useful to compare the behaviour of the relativistic potential with the standard Newtonian expression:

$$V_{\text{Newton}} = -\frac{M}{r} + \frac{L^2}{2r^2}. \tag{31}$$

This always approaches $+\infty$ as $r \to 0$; in other words, in the Newtonian case the centrifugal barrier always becomes infinitely tall as the central object is approached. This means that as long as a particle has any angular momentum, no matter how small, it will avoid hitting $r = 0$. However, notice that the relativistic potential always approaches $-\infty$ as we get closer to the center of the geometry. Hence, irrespective of the value of L the centrifugal barrier in the relativistic case is finite. If any particle's

path takes it too close to $r = 0$, it *will be irrevocably drawn to the central object*. This is our first indication of the immense attractive power of the body in the middle of the Schwarzschild geometry.

Radial infall Let us now concentrate on the case of purely radial motion of our test particle; i.e., $L = 0$. We are interested in the following question: if our particle is initially at $r = r_0 > 2M$ and has $\dot{r} < 0$, how long does it take for it to fall through the horizon? As stated, the question is somewhat ambiguous, because the issue of "how long?" depends on whose clock you are using. Let us first assume that the relevant clock is the one travelling with the particle. Then the quantity to calculate is

$$\Delta\tau = \int_{r_0}^{2M} \frac{dr}{\dot{r}} = \int_{2M}^{r_0} \frac{dr}{\sqrt{E^2 - f}}. \tag{32}$$

It is not difficult to convince oneself that this integral is finite for finite values of r_0, which means that an observer falling through the Killing horizon does so in a non-infinite amount of proper time. But there is another type of clock that we can consider, namely one that tracks the passage of the coordinate time t. What is the physical interpretation of t? Well, it is easy to see that for an observer at rest at $r = \infty$, t measures their proper time. So we can think of the coordinate time t as the time measured by an observer at rest very far away from $r = 0$. So according to such an observer, how long does the infall take? The answer is

$$\Delta t = \int_{r_0}^{2M} \frac{\dot{t}}{\dot{r}} dr = E \int_{2M}^{r_0} \frac{dr}{f\sqrt{E^2 - f}}. \tag{33}$$

One can confirm that this integral is always *divergent*. Therefore, it takes an infinite amount of coordinate time for an object to cross the Killing horizon $\mathcal{H}$, even though the same process occurs in a finite amount of proper time.

Which of these two measures of time are we to believe? Well, they are both correct given the proper interpretation: a comoving observer will measure a finite time interval while a stationary observer will measure an infinite interval. However, the strangeness of the later result may cause us to question the coordinate system we have been employing to this point. The proper time interval $\Delta\tau$ is a relativistic invariant and will be the same for all choices of coordinates. But Δt is tied to our choice of observers at infinity, and there is nothing particular sacred about that choice. The divergence of Δt for radial infall can be viewed as a hint that our coordinate system (t, r, θ, ϕ) has embedded in it some strange physics, and that there might be a better one out there for describing physics near $\mathcal{H}$.[5] This is not to say that our coordinates are not without some charm; they do highlight the asymptotic behaviour of the metric well and t does have a well-founded physical interpretation. Lesson: different problems often required different coordinates.

1.4.3 Null geodesics

The next topic to tackle is null geodesics. These are important because they define the path taken by light rays through our spacetime, and since nothing travels faster than light rays they also define the limiting behaviour massive particle trajectories.

The potential governing null geodesics is derived from (25) with $\kappa = 0$. The analysis for $L \neq= 0$ is similar to that of the massive case, so we will not repeat it here.[6] We will

[5] The (t, r, θ, ϕ) system is sometimes called Schwarzschild, or canonical coordinates.

[6] See Exercise 4.

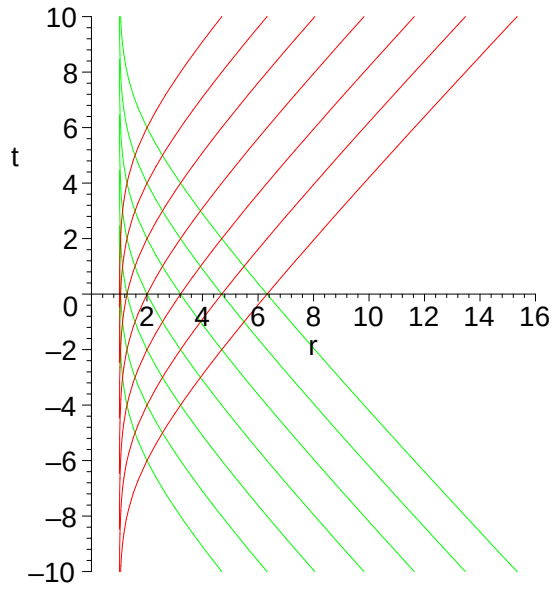

Figure 2: Ingoing (green) and outgoing (red) null geodesics in the Schwarzschild geometry for $M = 1/2$

instead immediately specialize to the $\dot{\phi} = 0$ case and work from first principles. Since massless particles (which we may generically call "photons", even though they could be something else) travel on trajectories with $ds^2 = 0$, we have:

$$0 = -f\,dt^2 + \frac{1}{f}\,dr^2 \quad \Rightarrow \frac{dt}{dr} = \pm\frac{1}{f}. \tag{34}$$

The equation on the right gives us a differential equation for t as a function of r. In other words, a convenient parametrization of radial null geodesics is with the r coordinate itself. We can solve for $t = t(r)$ by defining[7]

$$r_* = \int_r \frac{du}{f(u)} = r + 2M \ln\left(\frac{r}{2M} - 1\right). \tag{35}$$

Then, photons can travel on paths given by

$$\begin{aligned} u &\equiv t - r_* = \text{constant, or} \\ v &\equiv t + r_* = \text{constant.} \end{aligned} \tag{36}$$

Outside the horizon, the trajectories with $u =$ constant have $dr/dt > 0$ and are hence termed "outgoing" light rays, while the $v =$ constant curves have $dr/dt < 0$ and are called "ingoing" rays. In Figure 2, we have plotted some ingoing and outgoing rays in the (t, r) plane. From the plot, we see that the rays approach $t = \pm r +$ constant for large values of r, while they seem to asymptote to $r = 2M$ as they approach the central object. In fact, none of the rays actually seem to intersect $r = 2M$ for finite values of t. This is entirely analogous to the massive case, where we saw that it takes an infinite amount of coordinate time to fall through the horizon.

[7]The quantity r_* actually has a special name: the Regge-Wheeler tortoise coordinate.

Affine vs. non-affine parametrization The last point raises an interesting issue: in the massive case radial infall went on for a finite amount of proper time despite the divergence of Δt. We would like to convince ourselves that the same thing goes on for null geodesics, but we do not have an easily importable notion of proper time. After all, τ is really the arclength along a timelike curve and null geodesics have zero arclength by definition. However, it turns out that there is a good generalization of proper time to the null case; namely, the affine parameter.

To see how the concept of an affine parameter comes about, consider the tangent vector to the radial null paths we studied above:

$$k^\alpha = \frac{dx^\alpha}{dr}, \quad \left\{ \begin{array}{c} k^\alpha_{\text{out}} \\ k^\alpha_{\text{in}} \end{array} \right\} = \pm \frac{1}{f}\frac{\partial}{\partial t} + \frac{\partial}{\partial r}. \tag{37}$$

This tangent vector is obviously defined with respect to the r-parametrization. It is straightforward to show that the covariant acceleration of this vector is zero:

$$k^\alpha \nabla_\alpha k^\beta = 0. \tag{38}$$

Parameters which generate tangent vectors with zero acceleration are called affine parameters. So in this case, we see that r is an affine parameter along radial null geodesics. Therefore, when a photon travels from $r = r_0$ to to $r = 2M$ along a radial null geodesic, the change in the affine parameter λ is

$$\Delta\lambda = r_0 - 2M, \tag{39}$$

which is certainly finite, just as in the massive test particle case.

To see an example of a non-affinely parameterized geodesic, consider the same paths parameterized by the r_* coordinate defined above

$$\tilde{k}^\alpha \equiv \frac{dx^\alpha}{dr_*} = \frac{dr}{dr_*}\frac{dx^\alpha}{dr} = \pm\frac{\partial}{\partial t} + f\frac{\partial}{\partial r}. \tag{40}$$

The acceleration of this vector is

$$\tilde{k}^\alpha \nabla_\alpha \tilde{k}^\beta = \tilde{k}^\beta \frac{df}{dr}, \tag{41}$$

which in nonzero. Hence, r_* is a non-affine parameter for radial null geodesics.

The Killing horizon as a null surface We now move on to discover what null geodesics can tell us about the Killing horizon $\mathcal{H}$. When we look at Figure 2, it is hard not to notice that the null trajectories all approach the $r = 2M$ surface in the limit of $t \to \pm\infty$. In fact, the limiting case of both families of ingoing and outgoing rays seems to be $r = 2M$, which suggests to us that there are actually light beams that live on $\mathcal{H}$. This is in fact true, because we know that for null geodesics

$$\frac{dr}{dt} = \pm f. \tag{42}$$

Therefore, if a null ray starts on $\mathcal{H}$ where $f = 0$, we see that it will stay there for all t. In other words, $\mathcal{H}$ can be defined by the trajectory of a spherical shell of light that starts at $r = 2M$ and stays there forever. We say that $\mathcal{H}$ is *generated* by null geodesics and is hence a *null hypersurface*.

We can establish that $\mathcal{H}$ is a null surface in a different manner by considering the non-affine tangent vector $\tilde{k}^\alpha$ to the generating geodesics, which is sometimes called the *generator* of the horizon. It is straightforward to confirm that on $\mathcal{H}$ we have

$$\tilde{k}^\alpha = \pm\partial_t, \quad \tilde{k}_\alpha = dr. \tag{43}$$

Unlike its affine cousin k^α, we see that the components of $\tilde{k}^\alpha$ remain finite on $\mathcal{H}$, which makes it a more convenient tool to study the nature of the horizon. The first of these expressions implies that the integral curves of $\tilde{k}^\alpha$ run along $\mathcal{H}$, while the second implies that $\tilde{k}_\alpha$ is orthogonal to those same curves! It is a bizarre property of null surfaces that they are both tangent and normal to the vector fields that generate them.

Before moving on, we note that on $\mathcal{H}$, the Killing vector $\xi^\alpha_{(t)}$ is actually tangent to the null geodesics that generate the surface. This leads to a slightly more sophisticated definition of a Killing horizon:

> A **Killing horizon** is the null surface generated by the curves tangent to a null Killing vector field.

This definition is quite general and applies in a wide variety of spacetimes.

Gravitational redshift We now want to expand our discussion of null geodesics by interpreting them as the path taken by rays of light. We are in particular interested on how the properties of the vector tangent to null paths are related to the properties of the electromagnetic radiation they represent.

We first need to review a little special relativity. In that flat space theory, recall that the phase of an electromagnetic plane wave is

$$\phi = -\omega t + \mathbf{k}\cdot\mathbf{x}, \tag{44}$$

where the $(t, \mathbf{x})$ coordinates refer to some inertial frame S. The direction of propagation of the wave through spacetime is then given by the 4-dimensional wavevector

$$k_\alpha = \partial_\alpha\phi = -\omega\, dt + \mathbf{k}\cdot\mathbf{dx} \tag{45}$$

Now, an observer O at rest in the S frame will measure the frequency of the wave to be $k^0 = -\hat{t}_\alpha k^\alpha = \omega$, where $\hat{t}^\alpha = \partial_t$ is the observer's 4-velocity. Now consider a different observer O' moving with 3-velocity $\mathbf{v}$. The 4-velocity of such an observer is

$$u^\alpha = \frac{\partial_t + \mathbf{v}\cdot\nabla}{\sqrt{1-v^2}}. \tag{46}$$

According to the redshift formula of special relativity, the frequency of the wave as measured by O' is

$$\omega' = \frac{\omega - \mathbf{v}\cdot\mathbf{k}}{\sqrt{1-v^2}} = -u_\alpha k^\alpha. \tag{47}$$

So we see than in either frame, the measured frequency is simply minus the scalar product of the wavevector with the observer's 4-velocity.

We now want to import this result into the general theory, but we are faced with an ambiguity. Clearly, the wavevector of special relativity should be identified with the tangent vector to light rays in curved space, but what parametrization are we to adopt? In other words, do we take an affine parameter or do we take a non-affine parameter to

define k^α? The answer is again furnished by special relativity itself, where wavevectors to even non-planar electromagnetic radiation satisfy $k^\beta \partial_\beta k^\alpha = 0$.[8] Hence, in general relativity the frequency of a light ray measured by an observer with 4-velocity u^α is $-u_\alpha k^\alpha$, where k^α is the affine tangent vector to the ray's trajectory.

With this result in mind, we consider the following physical situation: two observers A and B are located at radii r_A and r_B in the Schwarzschild geometry, and we assume that each observer has no angular velocity. Observer A sends a radio signal to observer B that has frequency $\omega_{\rm A}$ in A's rest frame. We want to know what the frequency $\omega_{\rm B}$ of the signal is according to observer B as measured in his or her rest frame. The way that we have arranged things, the 4-velocities of both A and B are parallel to the timelike Killing vector field in the spacetime and can hence be expressed as

$$u^\alpha = \frac{\xi^\alpha_{(t)}}{\sqrt{-g_{\mu\nu}\xi^\mu_{(t)}\xi^\nu_{(t)}}}. \tag{48}$$

Then, we have

$$\omega_{\rm A} = -u_\alpha k^\alpha\big|_{r=r_A}, \quad \omega_{\rm B} = -u_\alpha k^\alpha\big|_{r=r_B}, \tag{49}$$

where k^α is the affine null tangent vector. But note that since we have $k^\alpha \nabla_\alpha k^\beta = 0$, $g_{\alpha\beta}k^\alpha \xi^\beta_{(t)}$ is conserved along the ray. This allows us to write the ratio of the two frequencies as

$$\frac{\omega_{\rm A}}{\omega_{\rm B}} = \frac{\sqrt{-g_{\mu\nu}\xi^\mu_{(t)}\xi^\nu_{(t)}}\big|_{r=r_B}}{\sqrt{-g_{\mu\nu}\xi^\mu_{(t)}\xi^\nu_{(t)}}\big|_{r=r_A}} = \sqrt{\frac{f(r_B)}{f(r_A)}}. \tag{50}$$

Since f is a monotonically increasing function for $M > 0$, we have that $r_A < r_B$ implies $\omega_{\rm B} < \omega_{\rm A}$. Therefore, as radiation travels away from the central body it becomes red-shifted, and as it travels towards the body it becomes blue-shifted. This effect has a simple physical interpretation: the gravitational potential energy of test particles (including photons) is a monotonically increasing function of radius. Therefore, as a light ray increases its radius the energy stored in the oscillations of the electromagnetic field are converted into gravitational potential energy, hence the red-shifting effect.

If we push r_B to infinity and denote $\omega_{\rm B} = \omega_\infty$, then

$$\omega_{\rm A} = \mu(r_A)\omega_\infty, \quad \mu \equiv \frac{1}{\sqrt{-g_{\mu\nu}\xi^\mu_{(t)}\xi^\nu_{(t)}}} = \frac{1}{f^{1/2}}. \tag{51}$$

We call μ the redshift factor for the Schwarzschild geometry, and it physically represents the factor by which the frequency of electromagnetic radiation is increased over its value at infinity, as measured by constant $\{r, \theta, \phi\}$ observers. Notice that as $r \to 2M$, the redshift factor diverges. So radiation become infinitely blue-shifted as it approaches the horizon $\mathcal{H}$.

1.4.4 Accelerating observers

Stationary observers We now move away from freely-falling towards accelerating observers. We will limit the discussion to massive observers with affinely parameterized 4-velocities; as discussed in Exercise 2e, this means that $u^\alpha \nabla_\alpha u^\beta = a^\beta$ and $u^\alpha u_\alpha = -1$, where a^α is the 4-acceleration. Presently, we are interested is *stationary observers*, but

[8] See Exercise 5.

what exactly does that mean? Well a reasonable definition is an observer that measures no time dependence in the geometry, or gravitational fields, surrounding them. In other words, an observer thinks that he is stationary if their environment seems to be static. Geometrically, we already determined that the partial derivative of the metric in the direction of a Killing vector is zero; or in other words, the metric is unchanging in the direction of a Killing symmetry. Hence, our stationary observers ought to have 4-velocities parallel to the timelike Killing vector in our spacetime. Such observers are also called *Killing observers* because their trajectories are the integral curves of Killing vectors. These observers are in some sense preferred since their motion is in harmony with the symmetry of spacetime.

We already saw stationary observers in the last section, where we called them observers with constant $\{r, \theta, \phi\}$. Their 4-velocity is

$$u^\alpha = \mu \xi^\alpha_{(t)}. \tag{52}$$

What is the acceleration of such observers? [For clarity of notation, we drop the (t) subscript on the timelike Killing vector in this calculation and below.]

$$\begin{aligned} a^\alpha &= u^\beta \nabla_\beta u^\alpha \\ &= \mu \xi^\beta \nabla_\beta (\mu \xi^\alpha) \\ &= \mu^2 \xi^\beta \nabla_\beta \xi^\alpha + \mu \xi^\alpha \xi^\beta \nabla_\beta \mu \\ &= -\mu^2 \xi^\beta \nabla^\alpha \xi_\beta + \mu^4 \xi^\alpha \xi^\beta \xi^\lambda \nabla_\beta \xi_\lambda \\ &= \tfrac{1}{2} \mu^2 \nabla^\alpha \mu^{-2} \\ &= -\nabla^\alpha \ln \mu \\ &= \tfrac{1}{2} f^{-1} \nabla^\alpha f. \end{aligned} \tag{53}$$

In going from the third to fourth and fourth to fifth lines, we have made use of $\nabla_\alpha \xi_\beta = -\nabla_\beta \xi_\alpha$. The magnitude of the acceleration is $(a_\alpha a^\alpha)^{1/2} = \frac{1}{2} f^{-1} (\nabla_\alpha f \nabla^\alpha f)^{1/2}$ which diverges on $\mathcal{H}$. Therefore, an observer needs to subject to an *infinite* external force to remain stationary on the Killing horizon. Again, we see the extreme attractive power of the central object in the Schwarzschild geometry.

The final phenomena we consider concerning stationary observers involve the following hypothetical situation: An observer at infinity is holding on to an inextensible string attached to a test particle hovering above the Killing horizon $\mathcal{H}$. The question is: what is the force per unit mass at infinity a^α_∞ required to keep the test particle stationary? To answer, note that the energy (per unit mass) of the test particle can be defined as $E = -u_\alpha \xi^\alpha = 1/\mu$ in analogy with the freely-falling case. Now consider what happens if the observer at infinity pulls on the end of the string such that its covariant displacement is $s^\alpha = \epsilon \hat{r}^\alpha$. Here, $\hat{r}^\alpha = f^{1/2} \partial_r$ is a unit vector in the radial direction and ϵ is a small quantity. We interpret the term "inextensible" to mean that the proper length of the string does not change during this process, so the end of the string and the test particle also undergoes a displacement of s^α. The change in energy of the test particle is $\delta E = -\mu^{-2} s^\alpha \nabla_\alpha \mu$ while the work done per unit mass by the observer at infinity is $W = a^\alpha_\infty s_\alpha$. Equating the work done with the change in energy yields

$$a^\alpha = \mu a^\alpha_\infty. \tag{54}$$

Hence the force exerted at infinity differs from the force exerted locally by the end of the string differs by a factor of the redshift. Now consider the case where the test particle is

right on the Killing horizon. Then, the magnitude of the force per unit mass at infinity is

$$\kappa = \sqrt{g_{\alpha\beta} a^\alpha_\infty a^\beta_\infty} = \frac{1}{2}\frac{df}{dr} = \frac{1}{4M}. \tag{55}$$

Thus, the force at infinity is finite despite the fact that the locally applied force is infinite. The quantity κ is known as the surface gravity of the horizon $\mathcal{H}$ since it characterizes the strength of the gravitational force at $r = 2M$.

Doomed (but still kicking) observers Notice that the redshift factor $\mu = f^{-1/2}$ is undefined for $f < 0$; i.e., inside the horizon. This means that the 4-velocity of stationary observers $u^\alpha = \mu \xi^\alpha_{(t)}$ does not even exist inside $\mathcal{H}$, which leads us to conclude that *there can be no stationary observers inside the horizon.* We can confirm this conclusion in a completely different way: Consider an arbitrary accelerating observer inside the horizon. If the observers 4-velocity is u^α, we have

$$u^\alpha u_\alpha = -1 \quad \Rightarrow \quad \dot{r}^2 = -f[1 + r^2(\dot{\theta}^2 + \sin^2\theta\dot{\phi}^2) - f\dot{t}^2]. \tag{56}$$

When $f < 0$, the quantity in the square brackets is greater than unity, which means that for our observer:

$$\left|\frac{dr}{d\tau}\right| \geq (-f)^{1/2} = \sqrt{\frac{2M}{r} - 1}. \tag{57}$$

This confirms that inside the horizon, it is impossible to have $dr/d\tau = 0$. In other words, an observer inside the horizon can

- never be stationary in the r direction, and
- never change the sign of their r-velocity.

This has several implications. First, there can be no static body of finite size existing within the horizon. If there were, the individual pieces of that body would have to following timelike paths with $\dot{r} = 0$, which do not exist. Stated in another way, it is impossible to have a finite body with enough structural integrity to remain static inside the horizon. Hence, we can conclude that if the central body in the Schwarzschild geometry has a radius less than $2M$ it can have no finite extent — all the mass must be concentrated at the central singularity. Second, if an observer crosses the horizon with $dr/d\tau < 0$, there is no way for them to avoid hitting $r = 0$. One may now be tempted to call the central object a "black hole" because we see that if anything massive falls through the horizon, it can never re-emerge. However, there is one point that one needs to keep in mind: our physical situation is entirely time reversible, hence the reverse of any admissible process is also admissible. So if a particle can fall into the horizon and hit the central singularity, a particle can also be emitted at $r = 0$ and travel to infinity. This is a quirk of an eternal geometry like the Schwarzschild case, where the central singularity is in existence for all time — below we will see that for a black hole of finite lifetime there can be no communication between the region inside the horizon and the exterior.

1.5 Causal structure and different coordinate systems

In the last section, we discussed a number of strange phenomena associated with the Killing horizon $\mathcal{H}$:

- It takes an infinite amount of time, as measured by an observer at infinity, for a massive particle to fall from a finite height to the horizon. This is despite the fact that according to an observer comoving with the particle, the time interval is finite.
- In the (t, r) coordinates, radially propagating ingoing or outgoing null geodesics asymptote to $\mathcal{H}$, but never seem to cross it; yet, the affine length of a null trajectory connecting $r_0 > 2M$ and $\mathcal{H}$ is merely $r_0 - 2M$.
- $\mathcal{H}$ is itself a null surface that radial null geodesics are confined to.
- The gravitational blueshift of electromagnetic radiation becomes infinite on the horizon.
- Stationary observers have an infinite acceleration when located at $\mathcal{H}$, and do not even exist when $r < 2M$.

We will soon see that some of these effects are tied to our choice of coordinates, while others are an intrinsic feature of the Schwarzschild geometry. To reach this level of understanding, we need to look at the metric in different coordinate systems.

1.5.1 Kruskal coordinates

Our main problem is that we do not have a coordinate system that is regular at the horizon. So, when we observe that timelike or null paths do not intersect the horizon for any finite value of t, it would be incorrect to assume that they never cross the horizon. Rather, it is entirely possible that they cross $r = 2M$ at some place in the manifold not covered by the Schwarzschild coordinates. This is supported by the fact that there is a coordinate singularity at $\mathcal{H}$ in the metric when expressed in the (t, r) frame; how can coordinates be used to describe a place where the metric is so badly behaved?

But how are we to construct coordinates that are well-behaved at the horizon? There are several ways to do this, but one of the best is based on the geodesics of the manifold. The rationale for this strategy is as follows: geodesics are solutions of a covariant equation of motion $u^\alpha \nabla_\alpha u^\beta = 0$ and are hence coordinate independent objects. If we have a coordinate singularity in our manifold that is not a genuine curvature (or some other type of) singularity, we expect geodesics to be "well-behaved" there; i.e., they are properly defined, smooth, differentiable, etc. Perhaps then, if we engineer a coordinate system based on geodesics we will have a metric regular across the offending location. Of course, this procedure can fail spectacularly, especially if what we thought was just a coordinate singularity is actually more serious — the only way to find out is by trying.

Now, we need to clarify exactly what we mean by coordinates based on geodesics. Well, recall we saw above that null geodesics travel on lines of u and v equal to constants, where

$$u = t - r_*, \quad v = t + r_*. \tag{58}$$

Also recall that r_* was the solution of the differential equation:

$$\frac{dr_*}{dr} = \frac{1}{f} \quad \Rightarrow \quad r_* = r + 2M \ln \left| \frac{r}{2M} - 1 \right|. \tag{59}$$

This is actually slightly different than the expression for r_* we wrote above (35) in that we have put absolute value bars around the argument of the logarithm. This expression

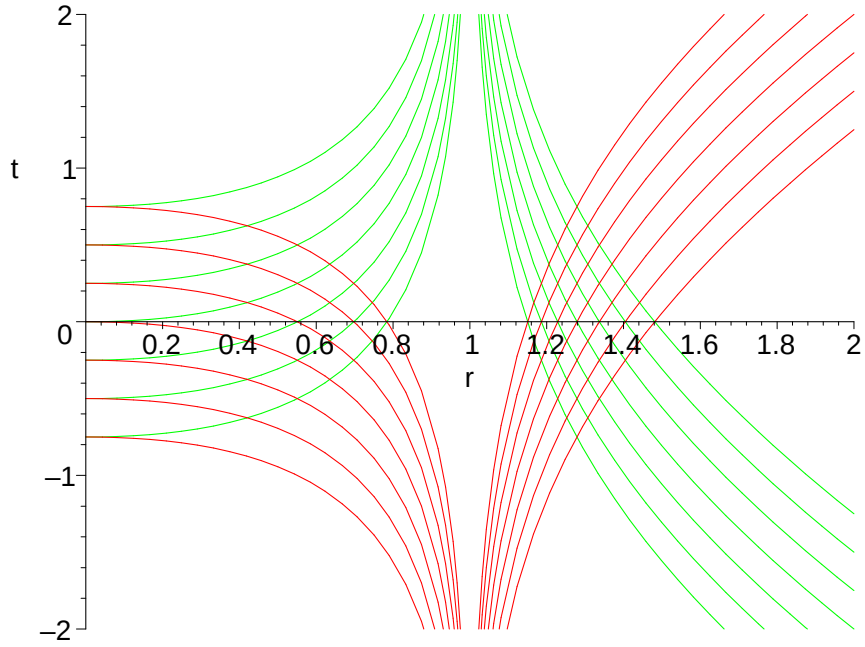

Figure 3: Lines of constant u (red) and v (green) in the (t, r) plane for the $M = 1/2$ case

for r_* is defined both inside an outside the horizon, which means that both u and v are properly defined as well. Now, if we wanted to construct a coordinate system "based on" null geodesics, it is clear that we should use u and v as coordinates instead of t and r. To get a geometric sense of that this entails, consider Figure 3. There, we have plotted lines of u and v = constant both inside and outside the horizon. It is clear that each point with $r \neq 0$ or $2M$ can be uniquely identified by the intersection of null geodesics, hence (u, v) is a viable coordinate system away from the curvature and coordinate singularities. This would seem to suggest that (u, v) cannot be the final answer to our search for a coordinate system regular across $\mathcal{H}$, but we will soon see that it is a valuable first step.

We won't be doing anything to the angular coordinates in this section, so to save writing we can just drop the $r^2\, d\Omega^2$ term from the metric. Now, we manipulate the metric as follows:

$$\begin{aligned} ds^2 &= -f\, dt^2 + f^{-1}\, dr^2 \\ &= -f(dt + f^{-1}\, dr)(dt - f^{-1}\, dr) \\ &= -f(dt + dr_*)(dt - dr_*) \\ &= -f\, du\, dv. \end{aligned} \tag{60}$$

Now consider

$$\frac{v-u}{4M} = \frac{r_*}{2M} = \frac{r}{2M} + \ln\left|\frac{rf}{2M}\right|. \tag{61}$$

This implies that

$$ds^2 = -\mathrm{sgn}(f)\, \frac{2Me^{-r/2M}}{r} e^{(v-u)/4M}\, du\, dv. \tag{62}$$

In this metric, the radius r should be viewed as an implicit function of u and v. Note that we cannot find an explicit expression for $r = r(u, v)$ because it is impossible to

find $r = r(r_*)$. Now in one regard, this representation of the metric is no improvement over the (t, r) version, because it is explicitly discontinuous across the horizon. But on the other hand, the metric coefficients approach finite values as $r \to 2M$; i.e., the discontinuity is finite and in some sense less serious than the coordinate singularity we had before.

If fact, it is a trivial matter to get rid of this discontinuity; we simply apply the following transformation:

$$U = -\mathrm{sgn}(f) e^{-u/4M}, \quad V = e^{v/4M}. \tag{63}$$

Then the metric becomes

$$ds^2 = -\frac{32M^3 e^{-r/2M}}{r}\, dU\, dV. \tag{64}$$

This metric is *totally* regular at $r = 2M$. There is simply no trace of singular behaviour on $\mathcal{H}$, which allows us to finally conclude that the Killing horizon is merely a coordinate singularity in the original Schwarzschild coordinates. However, the curvature singularity at $r = 0$ persists — no coordinate transformation can tame the divergent behaviour of the curvature scalars there. One further coordinate transformation puts the metric in the form originally put forth by Kruskal:

$$T = \frac{U+V}{2}, \quad X = \frac{V-U}{2} \quad \Rightarrow \quad ds^2 = \frac{32M^3 e^{-r/2M}}{r}(-dT^2 + dX^2). \tag{65}$$

As mentioned above, the coordinate transformation from (t, r) to (U, V) to (T, X) is of an implicit nature, so we cannot explicitly find $r = r(T, X)$ for example. But we do have the following relations:

$$UV = T^2 - X^2 = -e^{r/2M}\left(\frac{r}{2M} - 1\right), \tag{66a}$$

$$\frac{U}{V} = \frac{T-X}{T+X} = -\mathrm{sgn}(f) e^{-t/2M}. \tag{66b}$$

With these formulae, we have fully specified the transformation from the original Schwarzschild coordinates (t, r) to what are known as the *Kruskal-Szekeres coordinates* (T, X). When written in terms of the latter, the metric of the Schwarzschild geometry is utterly regular on the Killing horizon $\mathcal{H}$.

1.5.2 Maximal extension of the manifold and Kruskal diagrams

Glancing at the Kruskal-Szekeres line element (64), we note that it is well defined for all values of U and V such that $r > 0$.[9] Mathematically, this means that we must restrict

$$UV < 1. \tag{67}$$

[9] Actually, we could view the metric as being defined instead for all $r \in (-\infty, 0)$, but that makes our interpretation of r as proportional to the square root of the area of 2-spheres problematic. Note that the one thing we cannot do is allow for $r \in (-\infty, \infty)$ because the curvature singularity effectively forces us to choose one side of $r = 0$ or the other.

This is the only real restriction placed on the Kruskal-Szekeres coordinates by the metric. It is useful to give names to the various quadrants of the Kruskal-Szekeres plane:[10]

$$\begin{aligned}\text{Region I} &= \{(U,V) \in \mathbb{R}^2 | U < 0, V > 0, UV < 1\} \\ \text{Region II} &= \{(U,V) \in \mathbb{R}^2 | U > 0, V > 0, UV < 1\} \\ \text{Region III} &= \{(U,V) \in \mathbb{R}^2 | U < 0, V < 0, UV < 1\} \\ \text{Region IV} &= \{(U,V) \in \mathbb{R}^2 | U > 0, V < 0, UV < 1\}\end{aligned}$$

Now, our coordinate transformation (63) implies that the original Schwarzschild coordinates only cover the region I when $f > 0$, while region II is covered when $f < 0$. Hence, we see that the Kruskal coordinates cover a manifold that is in some sense *larger* than the original one we had envisioned when we derived the Schwarzschild solution. The situation is depicted in Figure 4, where we have drawn the t and r Schwarzschild coordinate lines according to the coordinate transformation (63). As implied by equations (69), the former are straight line segments emanating from the origin while the latter are hyperbolae. Clearly, these lines do not impinge on regions III or IV. However, notice that our original coordinate transformation (63) is not the only way to get from the (u, v) line element (62) to the Kruskal-Szekeres line element (64). Indeed, we could have easily defined[11]

$$U = \text{sgn}(f) e^{v/4M}, \quad V = -e^{-u/4M}. \tag{68}$$

In this case, (t, r) gets mapped onto region IV for $f > 0$ and region III for $f < 0$. Therefore, we can find Schwarzschild-like coordinates for all parts of the Kruskal diagram; but it should be stressed that the (t, r) coordinates only give a patchwork coverage. It is impossible to simultaneously describe more than one quadrant with Schwarzschild-like coordinates. Finally, note that equations (66) get modified to read:

$$UV = T^2 - X^2 = -e^{r/2M}\left(\frac{r}{2M} - 1\right), \tag{69a}$$

$$\frac{U}{V} = \frac{T - X}{T + X} = -\text{sgn}(f) e^{-\text{sgn}(V) t/2M}. \tag{69b}$$

From these considerations it is clear that we got more than we bargained for when we found a coordinate system that is regular across $\mathcal{H}$. The manifold described by the (T, X) coordinates not only contains the exterior and interior regions of the Schwarzschild geometry, it also contains one copy of each as well. Indeed, using equation (69) we see that the horizon $r = 2M$ actually corresponds to two different surfaces $T = \pm X$ in the Kruskal diagram. Even the singularity $r = 0$, which is described by $UV = 1$, corresponds to two different branches of a hyperbola. The complete manifold described by the Kruskal-Szekeres coordinates is known as the *maximal extension* of the Schwarzschild geometry.

A few other miscellaneous comments about Kruskal diagrams are in order:

- From the line element (64), we see that radial null geodesics travel on U or V equal constant lines. These correspond to $T = \pm X$; i.e., light rays travel on 45° lines in

[10] For anyone unfamiliar with this set notation, here is what our definition for region I sounds like in words: Region I is the collection of all points with both U and V in between $-\infty$ and $+\infty$, such that $U > 0$, $V > 0$ and $UV < 1$.

[11] This choice of coordinates is not unique: if we had instead selected $U = \text{sgn}(f) e^{u/4M}$ and $V = -e^{-v/4M}$ we would have had valid coordinates covering regions III and IV. However, this choice would have t running from top to bottom in IV, which would complicate the causality discussion below.

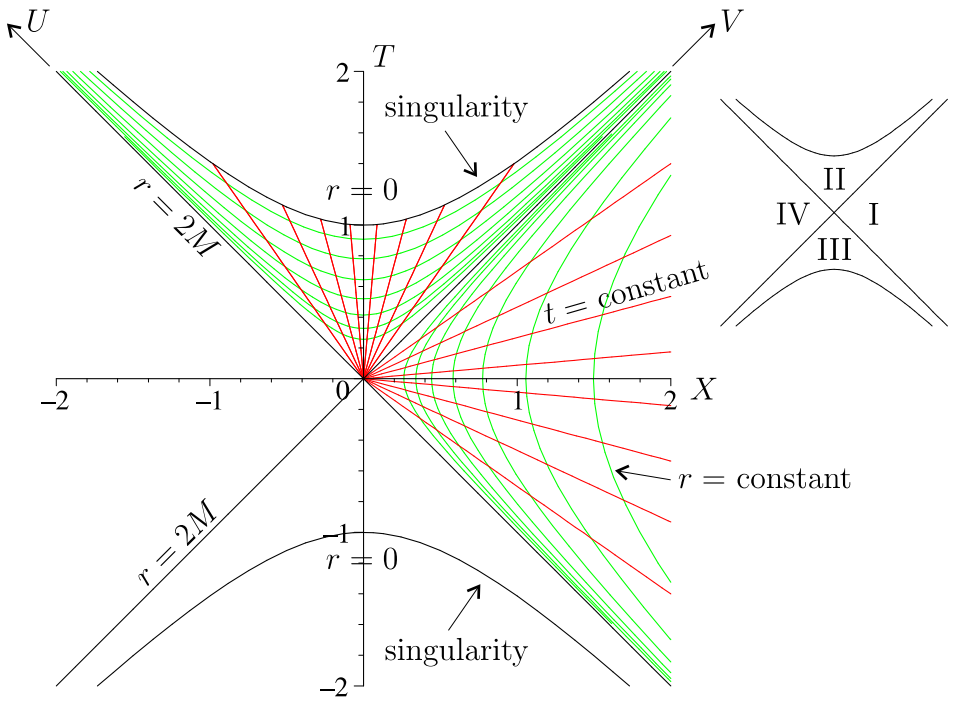

Figure 4: A Kruskal diagram of the (T, X) plane in the $M = 1$ case. We have drawn surfaces of constant t (red) and r (green) according to our original coordinate transformation (63). We see that in this case, the Schwarzschild coordinates only cover regions I and II of the extended manifold.

the Kruskal diagram. It also follows that timelike curves must have $|dT/dX| > 1$ (i.e., steep slopes) while spacelike ones have $|dT/dX| < 1$ (i.e., shallow slopes).

- In region I, which is the exterior region of the original Schwarzschild metric, the $t =$ constant lines are spacelike and the $r =$ constant curves are timelike, as one would intuitively expect. However, in region II the reverse is true; i.e., $t =$ constant is timelike and $r =$ constant is spacelike. This has everything to do with the fact that the timelike Killing vector $\xi^\alpha_{(t)}$ changes signature as one crosses $\mathcal{H}$, which implies that t and r exchange their roles as timelike and spacelike coordinates.

- If we restrict our attention to the (t, r) patch covering region I we see that the boundary between regions I and II corresponds to both $r = 2M$ and $t = +\infty$. On the other hand, the boundary between I and III is labelled as $r = 2M$ and $t = -\infty$. This vividly demonstrates the shortcomings of the (t, r) coordinates on the Killing horizon, where the time and radial coordinate lines are collinear and hence degenerate. It also explains why we never found any geodesics crossing the horizon at finite values of t; in a very real sense, for such trajectories the horizon is located at $t = \pm\infty$.

- Similarly, the Schwarzschild coordinates in IV (which is another exterior region) identify the boundary between IV and II as $(t = +\infty, r = 2M)$, and the boundary between IV and III as $(t = -\infty, r = 2M)$.

- The Schwarzschild coordinates in the exterior regions I and IV allow us to time ori-

ent our diagram by associating "past" with the bottom and "future" with the top. This makes the boundary between II and the two exterior regions the *future horizon* $\mathcal{H}^+$, and the boundary between III and the exterior regions the *past horizon* $\mathcal{H}^-$. Similarly, we call $T = \sqrt{1+X^2}$ the future singularity and $T = -\sqrt{1+X^2}$ the past singularity.

- Both $\mathcal{H}^+$ and $\mathcal{H}^-$ are null surfaces generated by outgoing and ingoing null geodesics, respectively.

1.5.3 Penrose-Carter diagrams

We have just seen how the maximally extended Schwarzschild geometry involves several distinct regions, each of which can be covered by a (t, r) coordinate patch. We now want to study how these regions are causally related to one another; i.e., can events in region II influence those in region III, or is it possible to send signals from region IV to region I? To answer these types of questions, it is useful to introduce yet another coordinate system, given by

$$\mathcal{U} = \frac{2}{\pi}\arctan U, \quad \mathcal{V} = \frac{2}{\pi}\arctan V. \tag{70}$$

The virtue of these coordinates is that they map $(U, V) \in \mathbb{R}^2$ onto $(\mathcal{U}, \mathcal{V}) \in \mathbb{U}^2$, where $\mathbb{U}$ is the finite interval $[-1, +1]$; i.e., instead of an infinite 2-dimensional plane we have a finite square to consider. In such cases, we refer to coordinates like $\mathcal{U}$ and $\mathcal{V}$ as *compactified* because they have finite ranges. The line element is then

$$ds^2 = -\frac{8\pi^2 M^3 e^{-r/2M}}{r}\sec^2\left(\frac{\pi\mathcal{U}}{2}\right)\sec^2\left(\frac{\pi\mathcal{V}}{2}\right)\,d\mathcal{U}\,d\mathcal{V}. \tag{71}$$

This has obvious coordinate singularities as $\mathcal{U}$ or $\mathcal{V}$ approaches ± 1, but these won't bother us too much we are more interested in the structure of the manifold as opposed to the behavior of the metric. Notice that this metric is actually identical to the Kruskal-Szekeres metric (64) except for a multiplicative prefactor. Metrics satisfying such a relationship are said to be *conformally identical*, and have the property that their null geodesics are the same. That is, null geodesics in the compactified metric are $\mathcal{U}$ or $\mathcal{V}$ equal to constant, whereas in (64) they are U or V equal to constant. Other than a trivial relabelling of coordinates, these curves are the same.

We need to know where the various special locations in the Kruskal diagram (4) get mapped to in these coordinates. In the Kruskal diagram, the future horizon was defined as $U = 0$ for $V > 0$ and $V = 0$ for $U > 0$, which translates into[12]

$$\mathcal{H}^+ = \{(\mathcal{U}, \mathcal{V}) \in \mathbb{U}^2 \,|\, \mathcal{U} = 0 \text{ for } \mathcal{V} > 0,\ \mathcal{V} = 0 \text{ for } \mathcal{U} > 0\}. \tag{72}$$

By the same token, the past horizon is given by

$$\mathcal{H}^- = \{(\mathcal{U}, \mathcal{V}) \in \mathbb{U}^2 \,|\, \mathcal{U} = 0 \text{ for } \mathcal{V} < 0,\ \mathcal{V} = 0 \text{ for } \mathcal{U} < 0\}. \tag{73}$$

How about the singularity $r = 0$? Recalling that $r = 0$ implied $UV = 1$ and using some simple trigonometry, we get:

$$1 = \frac{\cos\frac{\pi}{2}(\mathcal{U}-\mathcal{V}) - \cos\frac{\pi}{2}(\mathcal{U}+\mathcal{V})}{\cos\frac{\pi}{2}(\mathcal{U}-\mathcal{V}) - \cos\frac{\pi}{2}(\mathcal{U}+\mathcal{V})}. \tag{74}$$

[12] Again for anyone unfamiliar with set notation, in words this is: $\mathcal{H}^+$ is the collection of all points with both $\mathcal{U}$ and $\mathcal{V}$ in between -1 and $+1$, such that $\mathcal{U} = 0$ if $\mathcal{V} > 0$ and $\mathcal{V} = 0$ if $\mathcal{U} > 0$.

This is solved by

$$\mathcal{U}+\mathcal{V}=\pm 1. \tag{75}$$

This actually represents two surfaces in keeping with the fact that there is a bifurcation of $r=0$ in the Kruskal diagram. Now in the Kruskal diagram, the future singularity had both U and V positive, while the past singularity had U and V negative. This prompts the identifications

$$\text{future singularity} = \{(\mathcal{U},\mathcal{V})\in\mathbb{U}^2\,|\,\mathcal{U}+\mathcal{V}=+1\}, \tag{76}$$

$$\text{past singularity} = \{(\mathcal{U},\mathcal{V})\in\mathbb{U}^2\,|\,\mathcal{U}+\mathcal{V}=-1\}, \tag{77}$$

Note that these surfaces act as boundaries of the $(\mathcal{U},\mathcal{V})$-plane; i.e., the maximally extended Schwarzschild manifold exists in a region defined by $\{(\mathcal{U},\mathcal{V})\in\mathbb{U}^2\,|\,1>|\mathcal{U}+\mathcal{V}|\}$.

We need not stop with surfaces at finite values of (t,r). For example, consider *future timelike infinity*, which is defined as the point(s) on the manifold reached in the limit of $t\to\infty$ with $r\in(2M,\infty)$; i.e., r is outside the horizon but non-infinite. It physically represents the endpoint of timelike trajectories that do not intersect or asymptote to the horizon. Equations (63) imply that in region I the timelike trajectories approach

$$U\to 0,\ V\to+\infty. \tag{78}$$

On the other hand, in region IV (68) we have

$$U\to+\infty,\ V\to 0. \tag{79}$$

Hence, future timelike infinity is at

$$(\mathcal{U},\mathcal{V})=(1,0)\text{ or }(0,1). \tag{80}$$

In an entirely analogous way, define *past timelike infinity*, denoted by i^-:

$$t\to-\infty,\ r\in(2M,\infty)\quad\Rightarrow\quad(\mathcal{U},\mathcal{V})=(-1,0)\text{ or }(0,-1). \tag{81}$$

What if we were now to let $r\to\infty$ while holding t constant? Such a location should be rightly called *spacelike infinity*, denoted by i^0, and will satisfy

$$UV=-\infty,\ U=-e^{\mp t/2M}V\quad\Rightarrow\quad\mathcal{U}\to\pm1,\ \mathcal{V}\to\mp1. \tag{82}$$

Physically, spacelike infinity represents the large r limit of spacelike hypersurfaces.

There are two other types of infinity to consider: *future $\mathcal{I}^+$ and past $\mathcal{I}^-$ null infinity.* These are meant to be the end or initial points of outgoing or ingoing radial null geodesics respectively. Now, outgoing null geodesics travel on $u=$ constant curves, so they must end at $v=+\infty$. From the coordinate transformation valid in I (63), we have

$$V=e^{v/4M}\quad\Rightarrow\quad\mathcal{V}=1. \tag{83}$$

From the coordinate transformation in IV (68), we have

$$U=e^{v/4M}\quad\Rightarrow\quad\mathcal{U}=1. \tag{84}$$

In a similar way, for the ingoing geodesics past null infinity is at $u=-\infty$, which yields

$$\mathcal{U}=-1\text{ or }\mathcal{V}=-1. \tag{85}$$

Feature	r	t	u	v	$\mathcal{U}$	$\mathcal{V}$
future singularity	0^*	$\cdots$	$\cdots$	$\cdots$	$1-\mathcal{V}$	$1-\mathcal{U}$
past singularity	0^*	$\cdots$	$\cdots$	$\cdots$	$-1-\mathcal{V}$	$-1-\mathcal{U}$
future horizon $\mathcal{H}^+$	$2M^*$	$+\infty^*$	$+\infty$	finite	0 if $\mathcal{V}>0$	0 if $\mathcal{U}>0$
past horizon $\mathcal{H}^-$	$2M^*$	$-\infty^*$	finite	$-\infty$	0 if $\mathcal{V}<0$	0 if $\mathcal{U}<0$
future timelike infinity i^+	$>2M^*$	$+\infty^*$	$+\infty$	$+\infty$	0 or $+1$	$+1$ or 0
past timelike infinity i^-	$>2M^*$	$-\infty^*$	$-\infty$	$-\infty$	0 or -1	-1 or 0
spacelike infinity i^0	$+\infty^*$	finite*	$-\infty$	$+\infty$	± 1	∓ 1
future null infinity $\mathcal{I}^+$	$+\infty$	$+\infty$	finite*	$+\infty^*$	$\mathcal{U}=+1$ or $\mathcal{V}=+1$	
past null infinity $\mathcal{I}^-$	$-\infty$	$-\infty$	$-\infty^*$	finite*	$\mathcal{U}=-1$ or $\mathcal{V}=-1$	

Table 1: Location of special features in the maximally-extended Schwarzschild geometry. Primary definitions of each feature are indicated with an asterisk.

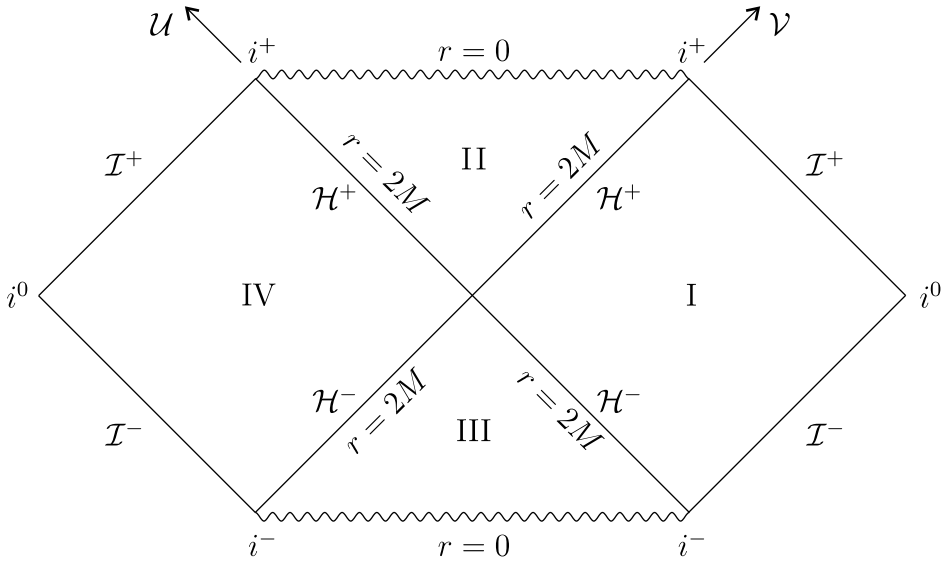

Figure 5: The Penrose-Carter (or conformal) diagram of the maximally extended Schwarzschild manifold

These are all of the infinities that we can think of. All of the characteristics of the special locations are summarized in Table 1.

Of course, a table is not the best way to get an appreciation of how these special features are related to one another. A diagram is the way to go, and this is what is given in Figure 5. This plot shows all of the features mentioned in Table 1 depicted in the $(\mathcal{U},\mathcal{V})$ plane. Since null geodesics travel on the $\mathcal{U}$ and $\mathcal{V}$ coordinate lines, we have oriented the $\mathcal{U}$ and $\mathcal{V}$ axes at an angle of 45°. Therefore, just as in the Kruskal diagram null geodesics travel on lines of slope 1. Timelike paths have $d\mathcal{U}\,d\mathcal{V}>0$, which implies a slope with an absolute value greater than 1. Similarly, spacelike curves have a slope lying in the interval $(-1,+1)$. Plots of this type are known as *Penrose-Carter* or *conformal* diagrams.

In Figure 6, we have redrawn the Penrose-Carter diagram with the Schwarzschild coordinate (t,r) coordinate lines shown in regions I and II. Some comments:

- as in the Kruskal diagram, $t=$ constant curves are spacelike and $r=$ constant curves are timelike in region I, while in quadrant II the reverse is true;

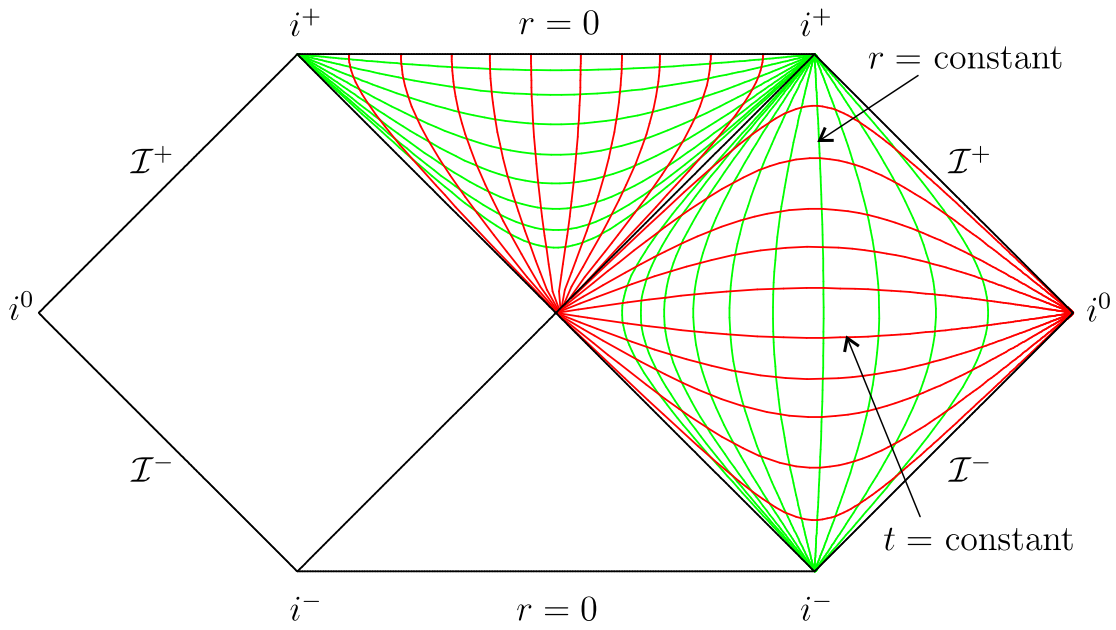

Figure 6: The Schwarzschild constant t (red) and r (green) lines drawn in regions of I and II in a Penrose-Carter diagram

- on the boundary $\mathcal{H}^+$ between I and II, both sets of coordinate curves become tangent to the null generators of the horizon;
- in region I, all timelike coordinate lines have terminal points on the timelike infinities i^- and i^+, while spacelike lines end at spacelike infinity i^0.

1.5.4 Interpreting the diagrams

We now use the Kruskal and Penrose-Carter diagrams to gain some understanding of the causal structure of the maximally extended Schwarzschild manifold, which is actually their main use.

Black holes and white holes Consider timelike paths that start in region I outside the $r = 2M$ region.[13] In a Penrose-Carter diagram, these have slope of modulus greater than unity. If we restrict our attention to ***future-directed*** paths with $dt/d\tau > 0$, we have that the direction of travel is generally upwards. Logically, these observers can either end up at i^+ or $\mathcal{I}^+$ in region I, or in region II. If they do cross $\mathcal{H}^+$ into II, then their ultimate fate can only be at $r = 0$. Similarly, any future directed null path starting in region I will end up on $\mathcal{I}^+$ or at $r = 0$. Therefore, we see:

> *Any future-directed timelike observer or light ray moving from region I to region II will collide with the singularity.*

Now, consider any timelike or null path beginning in region II. Note that we have no convenient notion of "future" or "past" in this part of the diagram because the $t =$

[13] Because of the symmetry of the extended Schwarzschild manifold, "region I" in this section can be interchanged with the other asymptotically flat "region IV."

constant lines are actually timelike; in other words, since t runs left-right instead of up-down, a timelike observer can switch from $\dot{t} > 0$ to $\dot{t} < 0$, or even have $\dot{t} = 0$. However if a timelike or null path travels from II to I, it will necessarily have $\dot{t} < 0$. Therefore:

> *It is impossible for a future-directed timelike or null trajectory to emerge from region II into region I.*

Consider the following definition:

> *The spacetime region A is said to be in the **causal future** of region B if one can find future-directed null or timelike geodesics travelling from B to A. In this situation, B is in the **causal past** of A.*

Intuitively, this definition implies that if A is in the causal future of B, an observer in A cannot send a signal or message to an observer in region B. Observers in A are then said to be ***out of causal contact*** with observers in region B. Then:

> *All of region I is in the causal past of region II, therefore any observer in II is out of causal contact with **any** observer in region I.*

So, if an observer falls through $\mathcal{H}^+$ from region I, other observers in region I will never hear from them again. By the same token, anything within region II cannot possible affect the course of events in region I. This motivates the following definition:

> *Consider two adjacent spacetime regions A and B. If all observers in A are out of causal contact with all observers in B, then the boundary between A and B is said to be an **event horizon** between A and B. Region A is said to be "behind the horizon." In this context, one can equivalently say that there is no overlap between A and the entire causal past of B.*[14]

Now, let us compare the conformal diagram of the Schwarzschild manifold with that of Minkowski space, shown in Figure 7. Notice that for Minkowski space, the entire diagram is in the past of future null infinity $\mathcal{I}^+$. In other words, it is always possible to send signals from any position in Minkowski space out to an observer at infinity, as long as one is willing to wait long enough. The Schwarzschild manifold is very different because the causal past of $\mathcal{I}^+$ does not include region II. At long last we have come to the notion of a black hole:

> *A spacetime manifold contains a **black hole region** if that region is not in causal contact with future null infinity $\mathcal{I}^+$.*

Physically, this definition just means that an observer entering a black hole region can never escape or send signals to infinity. Obviously, region II is a black hole region in the Schwarzschild manifold.

But if II is a black hole, then what is III? Region III is in casual contact with $\mathcal{I}^+$, but note that it is not in future of $\mathcal{I}^-$. Also note that:

> *It is impossible for any future-directed timelike or null path to enter region III from region I.*

So, while it is impossible to leave the black hole region II, we see that it is impossible to enter region III. This motivates the following definition:

[14] Defined to be complete set of spacetime points in the causal past of B.

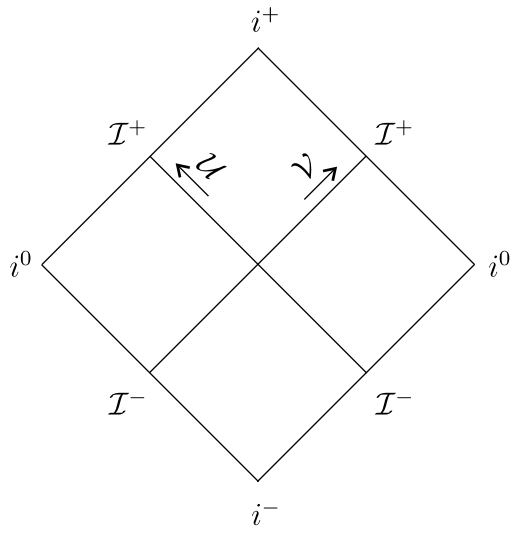

Figure 7: The Penrose-Carter diagram of Minkowski 2-dimensional space

> *A spacetime manifold contains a* ***white hole region*** *if that region is not in causal contact with past null infinity* $\mathcal{I}^-$*.*

Region III is therefore the white hole region of the Schwarzschild manifold.

We conclude the current discussion by addressing a common misconception concerning the Schwarzschild manifold: namely, that it is impossible for a anything to travel from the region with $r < 2M$ to the region with $r > 2M$. Such an idea naturally gives rise to the notion of a "black hole", but it unfortunately does not take into account the existence of the white hole. In the real Schwarzschild manifold, there is no problem finding a legitimate timelike trajectory starting at $r = 0$ in the white hole region, travelling through the "ordinary" part of the manifold with $r > 2M$, and then going off to infinity or entering the black hole region. This necessitates a more sophisticated definition of what a black hole is, and that is what we have given above.

The illusion of stalled radial infall Recall that above we saw that the radial infall of a massive particle through $\mathcal{H}$ seemed to take an infinite amount of coordinate time Δt. To some extent, we have already explained why this is the case: according to an observer using Schwarzschild coordinates, the future horizon $\mathcal{H}^+$ is located at $t = +\infty$ so it must take an infinite amount of coordinate time to reach it. *A priori*, Δt is a coordinate dependant quantity and is hence of dubious physical significance. We have argued that it is the amount of proper time for the infall as measured by an observer at infinity, but this is a rather vague notion. How exactly does such an observer make this measurement? After all, they are in an entirely different location than the particle, so how do they know what the infalling particle is actually doing or where it is? The answer is obvious: by looking at it; or rather, by making note of any radiation emitted or reflected by the particle towards their position. This realization allows us state the phenomenon in question in a more covariant manner:

> *An observer in one of the exterior regions (I or IV) will never see a test particle cross the future horizon* $\mathcal{H}^+$*. Rather, in the limit of late times such particles will appear to be frozen on the event horizon.*

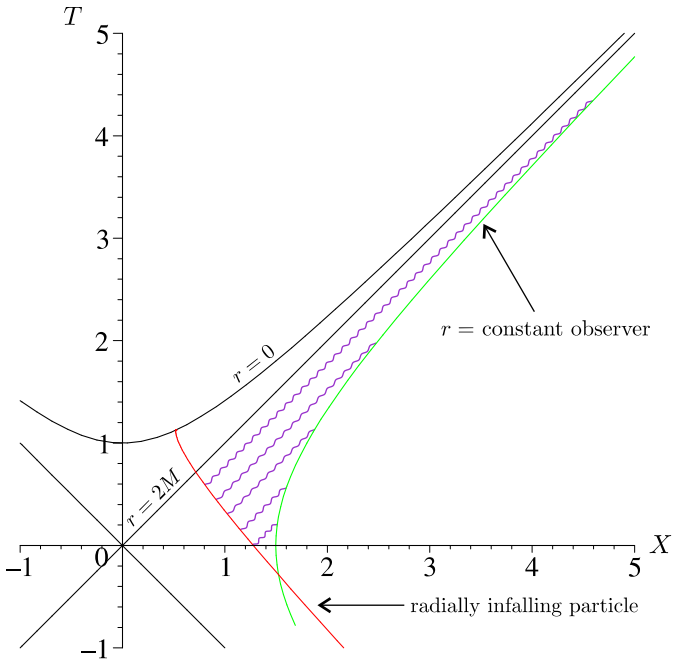

Figure 8: A Kruskal diagram depicting the radial infall of a massive particle (red worldline) as seen be a stationary observer (green worldline)

The "picture proof" of this statement is as follows: The physical situation we are considering is depicted in the Kruskal diagram of Figure 8. The worldline of the infalling particle is in red, while the green line represents the exterior observer.[15] The purple wavy lines represent light beams travelling from the infalling particle to the observer. First notice that even in the extreme future of the exterior observer, we can always find a purple line connecting them to the worldline of the test particle. So, our exterior observer will never loose sight of the particle. However, the purple lines can only intersect the red curve before it crosses $\mathcal{H}^+$. Therefore, the observer can only receive information about the particle before it enters the black hole region. Coupled with the fact that the observer will always be in causal contact with the particle, this proves that in the distant future the particle will appear to be effectively frozen on $\mathcal{H}^+$.

Parallel universes and wormholes One of the most intriguing things about the maximally extended Schwarzschild geometry is the existence of *two* asymptotically flat regions I and IV. In some sense, each of these represent distinct worlds, complete with separate observers, events, politics, etc. The two parallel universes are clearly causally disconnected from each other, so it is actually impossible to travel from one to the other without travelling faster than light. Lets consider why this is in more detail. Consider the spacelike surfaces A and B in the conformal diagram in Figure 9. Each of them span regions I and IV, so they represent the spatial geometry that must be crossed by anyone attempting to travel between the parallel universes. Now, the 3-geometries are actually dynamic in that they evolve with time; only surfaces orthogonal to the timelike Killing vector have static 3-geometries.

[15]Though it is not actually important for what we are doing, the red line in Figure 8 is the *actual* trajectory of a freely falling radial observer and the green line is a t = constant worldline.

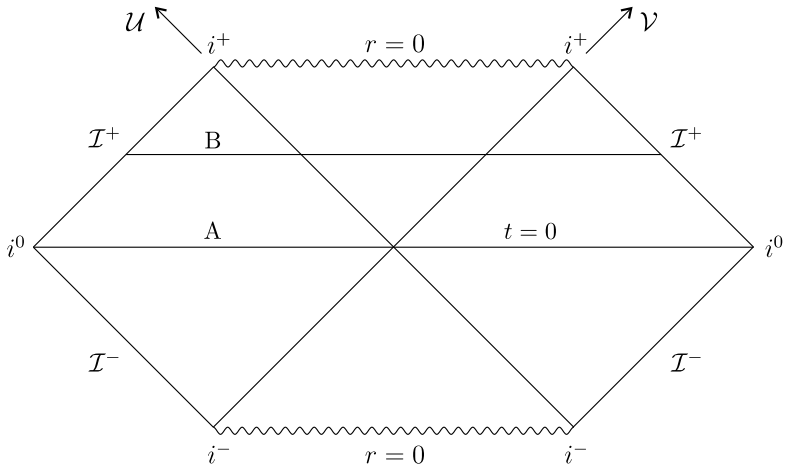

Figure 9: Some spacelike surfaces in the maximally-extended Schwarzschild manifold

What does the actual geometry of A and B look like? It is easiest to answer this for the $t = 0$ surface A because we have an explicit form for the 3-metric:

$$ds^2_{\rm A} = \left(1 - \frac{2M}{r}\right)^{-1} dr^2 + r^2\, d\Omega^2. \tag{86}$$

To get a feel for what the geometry is like, we can try to embed it as a 2-surface in flat 3-space. Obviously we can't embed a 3-dimensional surface in 3-space, so let's set $\theta = \pi/2$ such that each $r =$ constant surface is a circle of radius r:

$$ds^2_{\rm A} = \left(1 - \frac{2M}{r}\right)^{-1} dr^2 + r^2\, d\phi^2. \tag{87}$$

Now, consider flat 3-space written in terms of cylindrical coordinates:

$$ds^2_3 = dr^2 + r^2\, d\phi^2 + dz^2. \tag{88}$$

A surface of revolution in this space is defined by $z = z(r)$, and its geometry is:

$$ds^2_{\rm rev} = \left[1 + \left(\frac{dz}{dr}\right)^2\right] dr^2 + r^2\, d\phi^2. \tag{89}$$

Therefore, we can realize the geometry (87) by setting

$$\left(\frac{dz}{dr}\right)^2 = \left(1 - \frac{2M}{r}\right)^{-1} - 1 \quad \Rightarrow \quad z(r) = \pm\sqrt{8M(r-2M)}. \tag{90}$$

We have plotted this surface of revolution in Figure 10. In this plot, each of the horizontal circles represents a 3-sphere whose radius is the distance between the circle and the z-axis. Now in ordinary 3-dimensional space, if we have a set of 2-spheres concentric about some point we can always find one of the set with arbitrarily small radius. However, the concentric spheres the spacelike slice A does have a minimum: $r = 2M$. Stated in another way, it is impossible to draw a sphere of radius less than $2M$ around $r = 0$ in the $t = 0$ spatial 3-surface. As we travel radially along A towards $r = 2M$, which

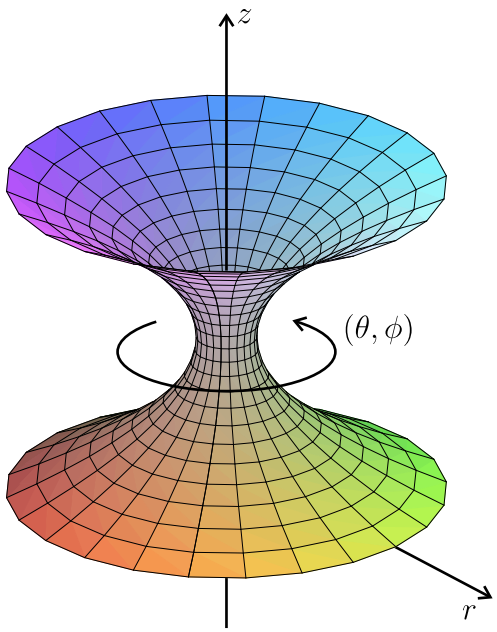

Figure 10: The $t = 0$ 3-surface embedded in flat space. The θ dimension has been suppressed, so each horizontal circle actually represents a 2-sphere. The radius of each sphere is just the distance between the circle and the z-axis.

correspond to travelling along the surface shown in Figure 10 in the z direction, the radii of spheres decreases until $r = 2M$ then starts to increase again. Inspection of the Penrose diagram in Figure 9 suggests what is happening: as we cross the $r = 2M$ 2-sphere on A, we are actually crossing from region I to region IV. In other words, the positive and negative z parts of the surface in Figure 10 represent completely different asymptotically flat regions. The spatial geometry of the $t = 0$ hypersurface is that of a *wormhole*; i.e., a bridge between "worlds." The "throat" of the wormhole is the smallest 2-sphere, and its radius is $2M$.

However, we know that this is not a traversable wormhole because regions I and IV are casually disconnected. When we were mentally "travelling" along the A 3-surface, we were doing so as spacelike observers. A real timelike observer will see a dynamic 3-geometry, with the initial A surface quickly evolving into the B surface in Figure 9. By looking at the constant r coordinate lines in Figure 6, it is not hard to convince oneself that the intrinsic geometry of B should be a lot like that of A, but the throat of the wormhole will have a radius of less than $2M$. As our observer continues to travel, the throat of the wormhole will get smaller and smaller. It is impossible for the observer to travel fast enough to get to the wormhole before it closes up completely; in fact, the only thing they will get for there troubles is a collision with the central singularity.

1.5.5 Eddington-Finkelstein coordinates and a redshift analogy

Even though the Kruskal coordinates have the virtue of covering the entire extended Schwarzschild manifold, they have the drawback of involving implicit functions like $r(U, V)$. This makes them difficult to use for actual calculations that require knowledge of the detailed geometry, as opposed to the causal structure. So, a more user-friendly

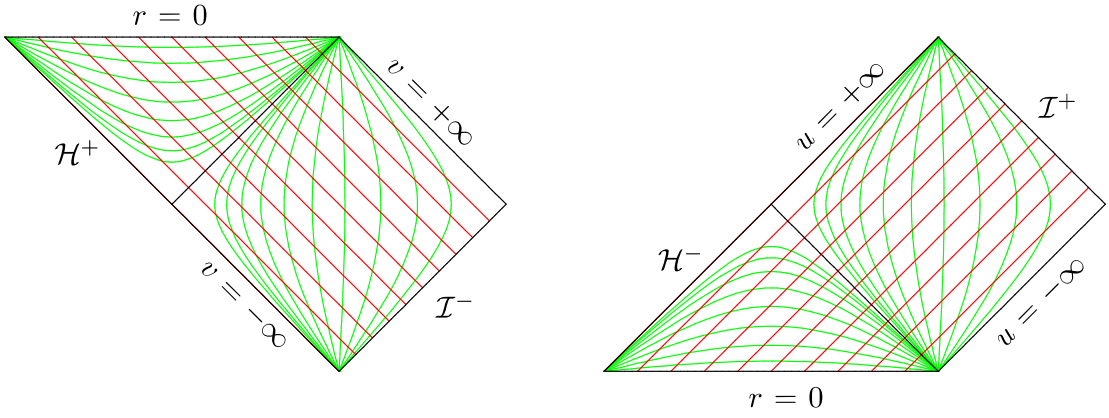

Figure 11: The portions of the maximally extended manifold covered by ingoing (*left*) and outgoing (*right*) Eddington-Finkelstein coordinates. Red curves are of constant constant v and u respectively, while green curves are of constant radius.

coordinate system is in order, but we still want a chart that is regular across the horizon. Luckily, we do not need to go particularly far to find one. Recall that the major problem with the Schwarzschild coordinates is the time parameter t; the horizon is located at $t = \pm\infty$, the time and radial coordinate lines become degenerate on $\mathcal{H}$, etc. So, what we were to use u or v instead of t? In such cases, using a procedure similar to the one in equation (60) we find:

$$ds^2 = -f\,du^2 - 2\,du\,dr, \tag{91a}$$
$$ds^2 = -f\,dv^2 + 2\,dv\,dr. \tag{91b}$$

We may be concerned that the f metric function still appears in this metric; doesn't this mean the inverse metric $g^{\alpha\beta}$ is singular on the horizon? Actually no, the non-diagonal nature of the metric saves us from any bad behaviour. For example, for the (v, r) coordinates:

$$g^{\alpha\beta}\partial_\alpha\partial_\beta = 2\partial_v\partial_r + f\,\partial_r^2, \tag{92}$$

which is manifestly finite.

In Figure 11, we plot the coverage of the (v, r) and (u, r) coordinates in a Penrose-Carter diagram. Because these coordinates are regular across $\mathcal{H}$, they are not confined to one quadrant like the Schwarzschild coordinates (t, r). On the other hand, they are obviously limited to $u \in (-\infty, +\infty)$ and $v \in (-\infty, +\infty)$. In quadrant I, this means that the former coordinates end on $\mathcal{H}^+$ and in the latter coordinates end on $\mathcal{H}^-$. So, the (u, r) coordinates cover regions I and III and the (v, r) coordinates cover regions I and II. Both of these coordinate systems were found and popularized by Eddington and Finkelstein, hence (u, r) are known as *outgoing Eddington-Finkelstein* coordinates and (v, r) are known as *ingoing Eddington-Finkelstein* coordinates, because of their regularity across $\mathcal{H}^-$ and $\mathcal{H}^+$ respectively.

One use of these coordinates is the construction of yet another type of spacetime diagram — namely Finkelstein diagrams. Concentrating on the ingoing coordinates for the moment, these are generally plots of $v - r$ versus r, as shown in Figure 12. The ingoing v = constant null curves travel on diagonal lines in these diagrams, but the

outgoing null curves travel on lines of varying slope given by

$$\frac{dv}{dr} = \frac{2}{f}. \tag{93}$$

Several thing are apparent from this diagram:

- When $r < 2M$, the outgoing rays are not outgoing at all, they are rather directed towards the singularity.
- The plot vividly demonstrates how $r = 2M$ actually is traced out by one of the "outgoing" rays. Since the ingoing coordinates are regular across $\mathcal{H}^+$ but not $\mathcal{H}^-$, $r = 2M$ must be identified with the future horizon in this picture. Hence, we explicitly see how the outgoing null geodesics generate $\mathcal{H}^+$.
- The bundle of arrows we have drawn at a few spacetime points in the diagram indicate the *future light cone* of massive test particles at that point. This is defined as the collection of possible directions that a timelike observer can follow from the given point, and is hence bounded by the ingoing and outgoing null rays. We see the famous "tipping of light cones" associated with the Schwarzschild geometry in the plot; i.e., when $r < 2M$ the light cones have all tipped towards the singularity, while for $r > 2M$ the cones still allow for $\dot{r} > 0$ motion.

Of course, one can construct similar diagrams for the outgoing (u, r) coordinates, but we won't do that here.

A redshift analogy One particularly interesting application of the outgoing coordinates is illustrated by the following physical situation: Suppose Alice is freely falling near a black hole. Her friend Barney is watching from very far away $r \gg 2M$ on a stationary trajectory. Alice carries with here a flashlight which she uses to send light pulses to Barney. Shes sends the pulses such that the time between pulses is $\Delta\tau$ in her rest frame. We want to know what is the time interval between pulses in Barney's rest frame.

If we use the outgoing Eddington-Finkelstein coordinates, then each of the outgoing pulses travels on a $u =$ constant curves. Consider two adjacent pulses travelling on $u = u_0$ and $u = u_0 + \Delta u$. Now, far away from the black hole $u \approx t - r$, so if Barney's trajectory is $r = r_B$, then the outgoing rays will hit Barney at $t_0 = u_0 + r_B$ and $t_0 + \Delta t = u_0 + \Delta u + r_B$. Since Barney is stationary, his proper time is just the t coordinate, hence in Barney's rest frame

$$\Delta t = \Delta u \tag{94}$$

is the time interval between pulses.

But how is Δu related to the time elapsed in Alice's rest frame? The answer comes simply from the radial geodesic equation, which yields (see Exercise 10):

$$\frac{du}{d\tau} = \frac{E \pm \sqrt{E^2 - f}}{f}, \quad \frac{dr}{d\tau} = \mp\sqrt{E^2 - f}, \tag{95}$$

where E is a constant. For infall, we choose the top sign in each formula. Hence, the time interval between pulses in Alice's frame is

$$\Delta\tau = \frac{f\Delta u}{E \pm \sqrt{E^2 - f}} = \frac{f\Delta t}{E \pm \sqrt{E^2 - f}}, \tag{96}$$

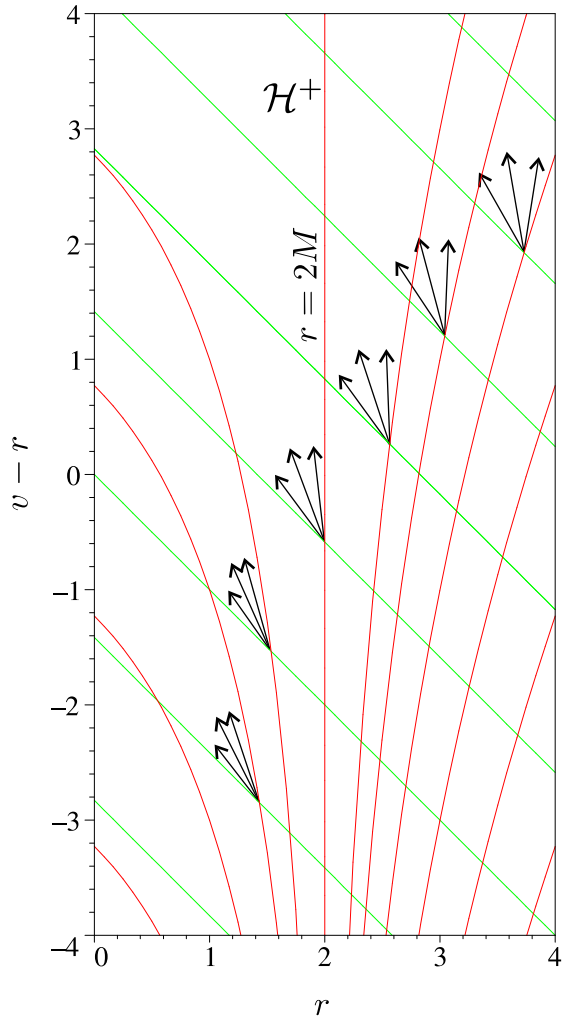

Figure 12: A Finkelstein spacetime diagram for $M = 1$ showing ingoing (green) and outgoing (red) null geodesics. The arrows indicate possible future directed worldlines of massive observers.

or

$$\omega_{\rm A} = \frac{E \pm \sqrt{E^2 - f}}{f}\omega_{\rm B}, \tag{97}$$

where $\omega_{\rm A}$ is the frequency of the light pulses in Alice's rest frame while $\omega_{\rm B}$ is the frequency in Barney's rest frame.

How do we interpret this? Well first consider the situation when Alice is nowhere near the black hole and is actually in the far field $r \gg 2M$ region. In this case:

$$\frac{du}{d\tau} = \frac{dt}{d\tau} - \frac{dr}{d\tau} \quad \Rightarrow \quad \frac{dr}{dt} = \mp\frac{\sqrt{E^2 - 1}}{E}. \tag{98}$$

Then, at infinity we have

$$\omega_{\rm A} = \frac{1 - \frac{dr}{dt}}{\sqrt{1 - \left(\frac{dr}{dr}\right)^2}}\omega_{\rm B}. \tag{99}$$

This exactly matches the special relativistic redshift formula (47) when we identify $\mathbf{v} = \frac{dr}{dt}\hat{\mathbf{r}}$ and $\mathbf{k} = \omega_{\mathrm{B}}\hat{\mathbf{r}}$, with $\hat{\mathbf{r}}$ as a radial unit vector. Therefore, our simple minded model has reproduced the redshift formula for light in flat space. In other words, we have seen that the redshift formulae in relativity need not be applied solely to electromagnetic radiation; rather they can be applied to any periodic signal emitted by one observer and received by another.

Let us confirm this result by considering the case when Alice is in the intermediate region $r \in (2M, \infty)$. Suppose that instead of her flashlight she has a laser of rest frequency ω_{A}. The laser light will have an affine tangent vector

$$k^\alpha = k^r \, \partial_r, \tag{100}$$

where k^r is some constant. The frequency in Alice's rest frame is

$$\omega_{\mathrm{A}} = -k_\alpha u^\alpha_{(\mathrm{A})} = k^r \frac{E \pm \sqrt{E^2 - f}}{f}. \tag{101}$$

Now, Barney's 4-velocity is $u^\alpha_{(\mathrm{B})} = \partial_u$, so he measures the frequency of the light received from Alice as

$$\omega_{\mathrm{B}} = -k_\alpha u^\alpha_{(\mathrm{B})} = k^r. \tag{102}$$

Putting together the expressions for ω_{A} and ω_{B} we recover our formula for periodic signals. Hence, we have shown that any periodic signal in general relativity can be treated using the redshift formulae for light.

Getting back to our original problem, we see that

$$\omega_{\mathrm{B}} \to 0 \text{ as } r \to 2M; \tag{103}$$

i.e., the frequency of light pulses seen by Barney will become infinitesimally small as Alice crosses the horizon, which mirrors the infinite redshift of radiation emitted from the near horizon region. We can interpret this by saying that each individual pulse of light takes longer to reach infinity than the previous one, with pulses emitted near $r = 2M$ having a nearly infinite travel time. The time delay of light signals induced by the gravitational field in the Schwarzschild geometry is the basis of one of the classic tests of general relativity, though light rays with non-zero angular momentum are conventionally employed.

1.5.6 Painlevé-Gullstrand coordinates: what does an observer falling into a black hole see and when do they get destroyed?

So far, all of the alternative coordinate systems that we have employed have been based on null geodesics. But we also have access to timelike geodesics, so it should be possible to construct a coordinate system regular across the horizon based on them. Above, we saw that it was sufficient to replace the t coordinate in order to get a well behaved chart; therefore, we should think of a way to measure time based on radially freely-falling observers.

There are several ways to do this, but we will adopt the following strategy: Consider the collection of all radially infalling observers that start from rest at infinity in the (t, r) plane; i.e., with $E = 1$. Draw a set of spacelike surfaces through the timelike geodesics such that they intersect orthogonally. Label each of these surfaces with a number $\mathcal{T}$. Then, we use T as our new time coordinate.

To go further, we need a few results from the theory of surfaces in differential geometry. On any spacetime manifold, a family of hypersurfaces can be defined by

$$\text{constant} = \mathcal{T}(x^\mu), \tag{104}$$

where changing the value of the constant picks out a particular member of the family. Now consider a small displacement s^α along one of the surfaces. Under such a displacement, our function $\mathcal{T}(x^\mu)$ must remain constant; i.e.,

$$0 = d\Phi = s^\alpha \partial_\alpha \mathcal{T}. \tag{105}$$

This implies that the vector $\partial_\alpha \mathcal{T}$ is orthogonal to any vector parallel to our family of hypersurfaces; i.e., $\partial_\alpha \mathcal{T}$ is proportional to the normal vector to the hypersurfaces.

Now, let u^α be the unit tangent vector to the radially infalling worldlines:

$$u^\alpha = \frac{1}{f}\frac{\partial}{\partial t} - \sqrt{1-f}\frac{\partial}{\partial r}. \tag{106}$$

Our construction implies that u^α should be orthogonal to the constant $\mathcal{T}$ surfaces, hence we should find $\mathcal{T}$ from the differential equations:

$$u_\alpha = -\partial_\alpha \mathcal{T}. \tag{107}$$

Actually, $u_\alpha = \mu \partial_\alpha \mathcal{T}$ would have sufficed, where μ is an arbitrary scalar function, but to keep things simple let's see if we can find a solution for $\mathcal{T}$ of this form.[16] It is actually fairly easy to solve this system to get:

$$\mathcal{T} = t + 4M\left(\sqrt{\frac{r}{2M}} + \frac{1}{2}\ln\left|\frac{\sqrt{\frac{r}{2M}}-1}{\sqrt{\frac{r}{2M}}+1}\right|\right). \tag{108}$$

This defines our new time coordinate. In terms of $\mathcal{T}$, the full metric is

$$ds^2 = -d\mathcal{T}^2 + \left(dr + \sqrt{\tfrac{2M}{r}}\, d\mathcal{T}\right)^2 + r^2\, d\Omega^2. \tag{109}$$

Owing to its discoverers, the $(\mathcal{T}, r)$ system is called Painlevé-Gullstrand coordinates. It is fairly easy to see that the metric and its inverse are regular across $r = 2M$.

In Figure 13, we show the coverage of the Painlevé-Gullstrand coordinates in a Kruskal and Penrose-Carter diagram assuming that when $r > 2M$, they cover region I; i.e., using the first Kruskal coordinate transformation (63). We see that they are regular across the future horizon, so the total coverage is of regions I and II. The spacelike nature of the $\mathcal{T}$ = constant lines is easier to see in the Kruskal diagram.

One of the main uses of the Painlevé-Gullstrand coordinates is the ease with which they allow us to answer the question: what does an observer "see" as they enter a black hole? We have several reasons to believe that the experiences of a freely falling observer near black hole may be somewhat fantastic. For example, we know that the time and space coordinates exchange character as one crosses $\mathcal{H}$ — does this means that if our observer one of the x, y, or z axes in our observers local rest frame will suddenly become timelike? We also saw in Figure 10 that the spatial geometry of Schwarzschild had a surprising structure; which causes us to wonder if read observers actually see the

[16] The minus sign is required to ensure that $\mathcal{T}$ increases towards the future.

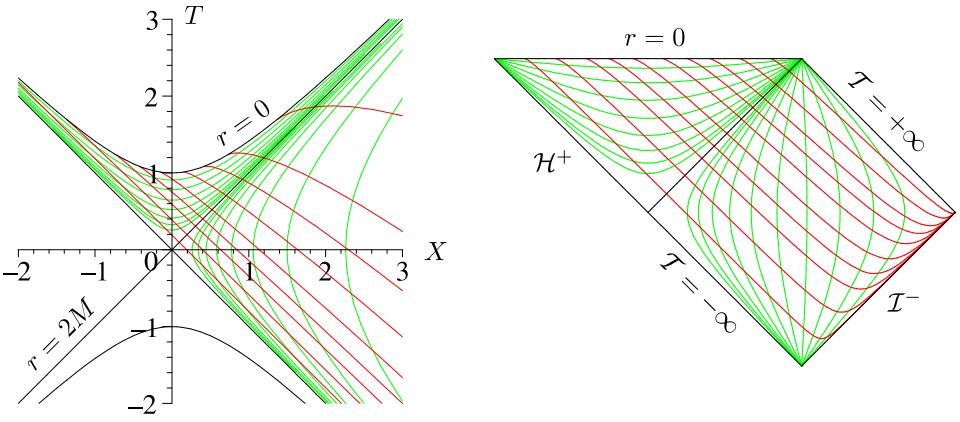

Figure 13: Constant $\mathcal{T}$ (red) and r (green) coordinate lines drawn in a Kruskal and Penrose-Carter diagram for the Painlevé-Gullstrand chart

geometry of a wormhole with a rapidly constricting throat as the approach the central singularity.

To address this issue, we need to more clearly specify what we mean by the spatial geometry "seen" by our observer. A natural definition is the 3-geometry in the observer's rest frame. For we know that in flat space, observers generally prefer to use spatial coordinates in which they are stationary. Geometrically, we can say that this preferred spatial geometry is that of the 3-surface orthogonal to the observers 4-velocity. Why? Because there is no projection of the 4-velocity onto that 3-surface, which means that the observer has no component of motion parallel to that surface; i.e., they are at rest with respect to that surface.

In our situation, the 3-geometry experienced by radially infalling observers is therefore that of the $\mathcal{T}$ = constant surfaces. But

$$ds^2_{(\mathcal{T})} = dr^2 + r^2\, d\Omega^2. \tag{110}$$

This is just flat 3-space! So the radially infalling observers do not see any pathological geometric phenomena as they go through the horizon or approach the singularity. There is no exchange of time and space, and they do not measure a wormhole geometry. This is one of the best confirmations we have seen that the geometry of Schwarzschild is regular across the horizon.

Tidal forces The conclusion an observer freely falling through the horizon measures a flat 3-geometry is perhaps surprising. It means that if an observer is in a closed vessel without windows, there is no way for them to determine if they have crossed $\mathcal{H}^+$ by performing local measurements. If they have a laboratory in their vessel, all physical experiments will be unaffected by the transition from region I to region II. But we have already seen that the "gravitational field" is certainly extreme in the near-horizon region — for instance, we know that it takes an infinite amount of local force to keep an object floating at $r = 2M$. Such a fact may have lead us to believe that the observers 3-geometry would be severely warped to reflect the strength of gravitational forces, but this is not the case.

For the same reasons, we might also be tempted to believe that the tidal force exerted on a finite body falling into the black hole would diverge at $r = 2M$. This

would certainly be true for a stationary test body of finite radial extent δr, since by equation (53) the difference between the magnitude of the gravitational force exerted on either end of the object is

$$\delta r \times \frac{\partial}{\partial r}\frac{M}{r^{3/2}(r-2M)^{1/2}} = -\delta r \frac{M(2r-3M)}{r^{5/2}(r-2M)^{3/2}}, \tag{111}$$

which clearly diverges as $r \to 2M$.[17] So a stationary body of finite size cannot exist arbitrarily close to the horizon, it would be ripped apart by extreme tidal forces. But what about the freely falling body? Does it similarly get destroyed in the near horizon region?

There is actually a very elegant way of describing the tidal forces experienced by a freely falling body in general relativity, which we will now describe. Consider some body moving in curved space in the absence of external forces. Suppose that in a certain frame of reference there is some axis running though the body on which we place a continuous parameter s. The s-axis is considered to be rigidly attached to the body, so that if the body is deformed the axis is similarly deformed. Hence, s supplies a label for each part of the object pierced by the axis. Now, we can specify the trajectory of each individual part of the body intersecting the s-axis by a function $x^\alpha = x^\alpha(\tau, s)$. For any given value of s, τ is a parameter along the worldline of the corresponding part of the body. We define the following vectors:

$$u^\alpha = \frac{\partial x^\alpha}{\partial \tau}, \quad \eta^\alpha = \frac{\partial x^\alpha}{\partial s}. \tag{112}$$

Now, we have some freedom in choosing both the frame of reference in which the s-axis is defined, as well as the parameter τ along the each of the worldlines. Immediately, we can use the latter to select

$$u \cdot u = -1; \tag{113}$$

i.e., τ is the proper time along each worldline. We will first consider the case where there are no internal forces that prevent the object from being deformed by the force of gravity.[18] Under these circumstances, each part of the body is freely falling and

$$0 = u^\alpha \nabla_\alpha u^\beta. \tag{114}$$

We have the following identity:

$$\begin{aligned} u^\alpha \nabla_\alpha \eta^\beta - \eta^\alpha \nabla_\alpha u^\beta &= u^\alpha \partial_\alpha \eta^\beta - \eta^\alpha \partial_\alpha u^\beta \\ &= \frac{\partial x^\alpha}{\partial \tau}\frac{\partial}{\partial x^\alpha}\frac{\partial x^\beta}{\partial s} - \frac{\partial x^\alpha}{\partial s}\frac{\partial}{\partial x^\alpha}\frac{\partial x^\beta}{\partial \tau} \\ &= \frac{\partial^2 x^\beta}{\partial \tau\, \partial s} - \frac{\partial^2 x^\beta}{\partial s\, \partial \tau} \\ &= 0. \end{aligned} \tag{115}$$

This allow us to show that the angle between u^α and η^α is conserved along each worldline:

$$\begin{aligned} u^\alpha \nabla_\alpha (u^\beta \eta_\beta) &= \eta_\beta u^\alpha \nabla_\alpha u^\beta + u^\beta u^\alpha \nabla_\alpha \eta_\beta \\ &= u^\beta \eta^\alpha \nabla_\alpha u_\beta \\ &= \tfrac{1}{2}\eta^\alpha \nabla_\alpha (u^\beta u_\beta) \\ &= 0. \end{aligned} \tag{116}$$

[17] The minus sign reflects the fact that the force of gravity decreases with increasing r.

[18] This would be the case if the "body" in question were a cloud of dust, for example.

Now, we still haven't specified in which frame of reference the s-axis is defined. Let us rectify this by considering the object's rest frame at a particular moment in time. In this frame, each part of the object has no spatial velocity; hence, if we define the s-axis as a purely spatial curve in this frame, η^α will be orthogonal to the 4-velocity u^α of each part of the body. By the above calculation, this means that $u \cdot \eta = 0$ for all other times as well.

What then is the geometric interpretation of η^α? Well, if we consider neighboring parts of the body located at s_0 and $s_0 + \delta s$, the vector $\eta^\alpha \, \delta s$ is the spatial displacement vector between the two points in the object's rest frame. We can therefore define the relative velocity between the two parts as the "time derivative" of η^α; i.e., $u^\alpha \nabla_\alpha \eta^\beta$. The relative acceleration is then

$$\begin{aligned} a^\alpha_{\text{rel}} &= u^\beta \nabla_\beta (u^\gamma \nabla_\gamma \eta^\alpha) \\ &= u^\beta \nabla_\beta (\eta^\gamma \nabla_\gamma u^\alpha) \\ &= (u^\beta \nabla_\beta \eta^\gamma)(\nabla_\gamma u^\alpha) + u^\beta \eta^\gamma \nabla_\beta \nabla_\gamma u^\alpha \\ &= (\eta^\beta \nabla_\beta u^\gamma)(\nabla_\gamma u^\alpha) + u^\beta \eta^\gamma (\nabla_\gamma \nabla_\beta u^\alpha - R^\alpha{}_{\mu\gamma\beta} u^\mu) \\ &= (\eta^\beta \nabla_\beta u^\gamma)(\nabla_\gamma u^\alpha) + \eta^\gamma \nabla_\gamma (u^\beta \nabla_\beta u^\alpha) - (\eta^\gamma \nabla_\gamma u^\beta)(\nabla_\beta u^\alpha) - R^\alpha{}_{\mu\gamma\beta} u^\mu \eta^\gamma u^\beta \\ &= -R^\alpha{}_{\mu\gamma\beta} u^\mu \eta^\gamma u^\beta. \end{aligned} \tag{117}$$

In going from the first to second line we made use of (115), from the third to fourth line we again used (115) along with the defining property of the Riemann tensor:

$$\nabla_\beta \nabla_\alpha A^\mu - \nabla_\alpha \nabla_\beta A^\mu = -R^\mu{}_{\nu\alpha\beta} A^\nu, \tag{118}$$

and from the fifth to sixth line we used the geodesic equation and relabelled dummy indices. Hence, the relative acceleration between neighboring parts of a freely falling body is

$$a^\alpha_{\text{rel}} = -R^\alpha{}_{\beta\gamma\delta} u^\beta \eta^\gamma u^\delta, \tag{119}$$

provided that the body has negligible structural integrity. The vector η^α represents the displacement between the two points under consideration.[19]

Now we consider a freely falling rigid body, where the relative velocity and acceleration inside the object is identically zero. While the body as a whole follows a geodesic trajectory, the lack of relative acceleration implies that individual parts of the object are subject to non-zero internal forces. Clearly, the internal forces have to exactly overcome the relative acceleration induced by gravity a^α_{rel}. Hence, we see that a^α_{rel} represents the gravitational tidal stress on a freely-falling rigid body in the direction of η^α.

Let's get back to the case of an object of finite size falling through the horizon of the black hole. In the Painlevé-Gullstrand coordinates, we can take:

$$u_\alpha = -d\mathcal{T}, \quad \eta^\alpha = \partial_r. \tag{120}$$

These vectors satisfy

$$1 = -u \cdot u = \eta \cdot \eta, \quad 0 = u^\alpha \nabla_\alpha u^\beta. \tag{121}$$

So u^α is the object's 4-velocity and η^α is an an orthogonal vector in the radial direction. A simple calculation reveals the gravitational tidal stress on the object in the radial direction as

$$a^\alpha_{\text{rel}} = \frac{2M}{r^3} \partial_r. \tag{122}$$

[19] Our formula for a_{rel} is also known as the equation of geodesic deviation because it characterizes the tendency for nearby geodesics to be attracted or repelled from one another.

The is finite at $r = 2M$, so we see that objects of sufficient internal strength can indeed survive the trip though the horizon. However this does diverge at $r = 0$, which suggests that any "realistic" finite body with finite structural integrity will be ripped to pieces before reaching the singularity.

2 Dynamical black holes

Up until this point, we have assumed that the Schwarzschild geometry describes an object that is eternal; i.e., has existed for all time and will continue to exist into the infinite future. This is obviously not the most physical scenario, so in this section we will consider dynamical black holes; i.e., black holes with non-trivial time dependence. Actually, there is precious little we can say about such objects at the analytic level because of the complexity of the field equations, so a certain portion of what we say will be somewhat qualitative.

2.1 The Vaidya geometry and apparent horizons

One of the most naïve ways in which we can make the Schwarzschild metric time dependent is to replace M with $M(t)$. Somewhat surprisingly, this is almost how we obtain the Vaidya metric, which described a black hole that is either emitting or being irradiated by "null dust." The ingoing Vaidya metric is obtained by replacing M by $M(v)$ in the ingoing Eddington-Finkelstein metric:

$$ds^2 = -f\,dv^2 + 2\,dv\,dr + r^2\,d\Omega^2, \quad f = 1 - \frac{2M(v)}{r}. \tag{123}$$

It is not difficult to calculate the stress-energy tensor for this metric:

$$8\pi T_{\alpha\beta} = \frac{2}{r^2}\frac{dM}{dv}\,\partial_\alpha v\,\partial_\beta v. \tag{124}$$

Now in this metric, the vector

$$k_\alpha = -\partial_\alpha v, \quad k^\alpha = -\partial_r, \quad k\cdot k = 0, \quad k^\alpha \nabla_\alpha k^\beta = 0, \tag{125}$$

is tangent to ingoing null geodesics. Hence the Vaidya stress-energy tensor is

$$T_{\alpha\beta} = \frac{1}{4\pi r^2}\frac{dM}{dv} k_\alpha k_\beta. \tag{126}$$

If k^α were timelike, we would interpret this as the stress-energy tensor of dust with density $\rho = \frac{1}{4\pi r^2}\frac{dM}{dv}$. However, k^α is actually null so we say that the ingoing Vaidya metric is sourced by radially infalling null dust. We require that the null dust has positive density:

$$\rho > 0 \quad \Rightarrow \quad \frac{dM}{dv} > 0. \tag{127}$$

Since $v = t - r_*$, this implies that the black hole mass increases in time. Conversely, working with the outgoing Eddington-Finkelstein coordinates with $M = M(u)$, we can derive the outgoing Vaidya metric sourced by radially outgoing null dust. The positivity of the density in that case requires a decreasing black hole mass $dM/du < 0$. Notice that in both cases, the functional dependence of M on v or u is arbitrary.

Apparent versus event horizons We now demonstrate that the Vaidya geometry requires us to refine our notion of what a "horizon" is. In the Schwarzschild metric we saw that the horizon $\mathcal{H}$ was a place:

- where the timelike Killing vector becomes null,
- where the outgoing null geodesics had zero radial velocity $dr/dt = 0$, and
- that constituted the boundary of regions causally disconnected from $\mathcal{I}^+$ or $\mathcal{I}^-$; i.e., an event horizon.

Now, it is easy to see that the outgoing Vaidya geometry does not even have a timelike Killing vector ∂_v unless $dM/dv = 0$. Therefore, there is no Killing horizon in the Vaidya geometry. On the other hand, we can define a horizon based on the locus of points where outgoing null geodesics have zero radial velocity. Because v takes the rôle of time in the ingoing Eddington-Finkelstein coordinates, such a horizon is defined by $dr/dv = 0$. For outgoing null rays, we have

$$\frac{dr}{dv} = \frac{f}{2}. \tag{128}$$

Hence, such a horizon corresponds to $f = 0$, or

$$r_{\rm AH} = 2M(v). \tag{129}$$

A horizon defined by the turning point of outgoing null geodesics is called an *apparent horizon*, hence the "AH" subscript.[20] Now consider a particle travelling along the apparent horizon with $(\theta, \phi) =$ constant. In the v-parametrization, the tangent to this particle's worldline is

$$u^\alpha_{\rm AH} = \partial_v + 2\frac{dM}{dv}\partial_r. \tag{130}$$

The norm of this tangent is

$$g_{\alpha\beta}u^\alpha_{\rm AH}u^\beta_{\rm AH} = 4\frac{dM}{dv} > 0; \tag{131}$$

i.e., the particle follows a *spacelike* trajectory. We can say that the apparent horizon is a spacelike surface for the Vaidya metric — in that all curves drawn along it are spacelike — whereas it is null for the Schwarzschild metric.

So what is the difference between the apparent and event horizons? This is actually best demonstrated by the consideration of a specific example. Suppose that, in dimensionless units, we have

$$M(v) = \begin{cases} 1, & v < 0, \\ \frac{1}{4}v + 1, & 0 < v < 1, \\ 2, & v > 4. \end{cases} \tag{132}$$

Physically, this choice of $M(v)$ corresponds to a static Schwarzschild black hole for $v < 0$ and $v > 1$. For $v \in (0, 1)$ the black hole is being irradiated by null dust and its mass increases linearly with v. The null dust stream can be thought to be switched on at

[20] A better definition in terms of the expansion of the outgoing null congruence is possible, but as we haven't developed the notion of what the expansion of a congruence is, we won't go into more detail.

$v = 0$ and switched off at $v = 1$. The apparent horizon is therefore given by a piecewise linear curve in a Finkelstein diagram:

$$r_{\rm AH}(v) = \begin{cases} 2, & v < 0, \\ \frac{1}{2}v + 2, & 0 < v < 1, \\ 4, & v > 4. \end{cases} \tag{133}$$

Now, where are the outgoing null geodesics in this spacetime? They follow trajectories given by

$$\frac{dr}{dv} = \frac{1}{2}\left[1 - \frac{2M(v)}{r}\right]. \tag{134}$$

It is actually possible to get a good handle on this equation analytically, but we opt for the quicker route of numeric integration. In Figure 14, we plot the apparent horizon (red) and several numeric solutions for the outgoing geodesics (green) in a Finkelstein diagram. As expected, the apparent horizon is piecewise linear, and when the null rays cross it with $dr = 0$; i.e., a vertical slope. All of the light rays shown begin outside the apparent horizon, yet three end up at $r = 0$ while two others escape to $r = \infty$. This should be compared with the Schwarzschild case shown in Figure 12, where the outgoing null geodesics never cross the apparent horizon at $r = 2M$. The fact that the apparent horizon can overtake null rays that are initially outside of it is testament to its faster-than-light spacelike growth. There is also one other null geodesic shown in Figure 14 that is somewhat special and drawn in black. This one neither escapes to infinity or falls into the singularity; rather it remains coincident with the apparent horizon for $v > 4$. It should be obvious that all of the points in the Finkelstein diagram to the left of the black curve are out of causal contact with $\mathcal{I}^+$, while the points to the right are. Hence the black curve is the event horizon in the Vaidya spacetime, and it is defined by a marginally trapped null geodesic.

Many of the qualitative properties of apparent and event horizons that we have discovered in our investigation of the Vaidya metric hold in more generic dynamical black hole manifolds. For example, the apparent horizon is always defined by the turning point of outgoing null geodesics and is always spacelike or null. The event horizon is always a causal boundary, and always lies outside the apparent horizon. An interesting application of all of this is in numeric relativity, where a simulation will often produce the metric of some interesting spacetime involving the collision of black holes, the collapse of realistic stars, etc. Of obvious interest is the location of the event horizon for such numerical solutions, but its very definition sometimes makes this hard to achieve. Again, this is best illustrated by an example. Consider a situation like before, but allow for a second period of null dust irradiation, say between $v = 10$ and $v = 14$. The behaviour of the apparent horizon and null geodesics is shown in Figure 15. We see that what was the event horizon in Figure 14 (now drawn in blue) is not the event horizon in the new scenario. The second period of irradiation increases the mass and hence gravitational attraction of the black hole, which pulls the blue null geodesic into the singularity. The true event horizon lies even further away from the apparent horizon in this case, and is drawn in black. The point is that in order to find the event horizon in a given spacetime we need to know its entire future evolution. If we were given a numeric simulation of the metric in Figure 15 that stopped before $v = 10$, we would incorrectly identify the blue curve as the event horizon. But numeric simulations always terminate at finite times, which means that finding event horizons from simulations is tricky at best. However, the apparent horizon is a quantity that is locally determined by the behaviour of null

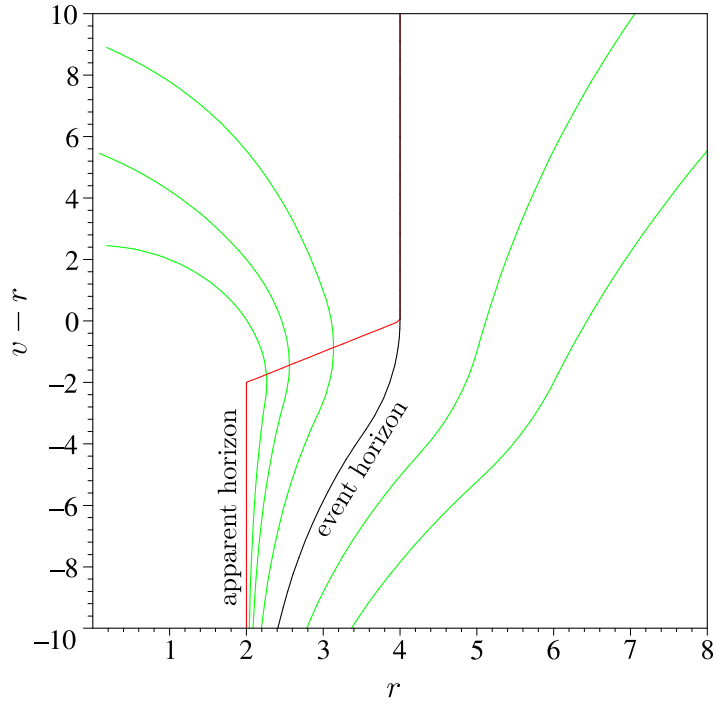

Figure 14: Outgoing null geodesics (green) in the Vaidya spacetime for the special case described in the text. Also shown is the apparent horizon (red) and the event horizon (black). Note that the event horizon is essentially defined by a marginally trapped null geodesic.

geodesics, and is relatively easy to access numerically. Hence, the output of most numeric work is the apparent horizon, not the event horizon.

2.2 The Birkhoff theorem

We continue our discussion of dynamical black hole spacetimes by considering the following situation: Suppose that we have some perfectly spherical distribution of matter that is both time-dependent and has a definite boundary. Outside of the boundary, we assume that there is a vacuum. An example of this situation is a idealized star undergoing gravitational collapse. We are interested in the solution of the vacuum Einstein equations outside of the object, and to obtain it we will need some sort of metric *ansatz*. Retracing the arguments of Section 1.1, we can take the 3-metric on each constant time slice of the exterior part of the manifold as[21]

$$ds^2_{(\bar{t})} = \bar{h}(\bar{t}, r)\, dr^2 + r^2\, d\Omega^2. \tag{135}$$

[21] In all honesty, the most general 3-dimensional line element is

$$ds^2_{(\bar{t})} = \bar{h}(\bar{t}, \ell)\, d\ell^2 + r^2(\ell)\, d\Omega^2.$$

However, we can always transform this into the form (135) *provided that* $dr/d\ell \neq 0$. Most situations do not involve $r(\ell)$ having local extrema, but we have already seen a notable exception in Section 1.5.4 with the $t = 0$ surface in the extended Schwarzschild manifold. The 2-spheres in that 3-surface did have a minimum area $4\pi(2M)^2$, signifying a minimum in $r(\ell)$ if the metric is written in the form above. However, even if $r(\ell)$ does have extrema, we can always adopt (135) in between those values of ℓ.

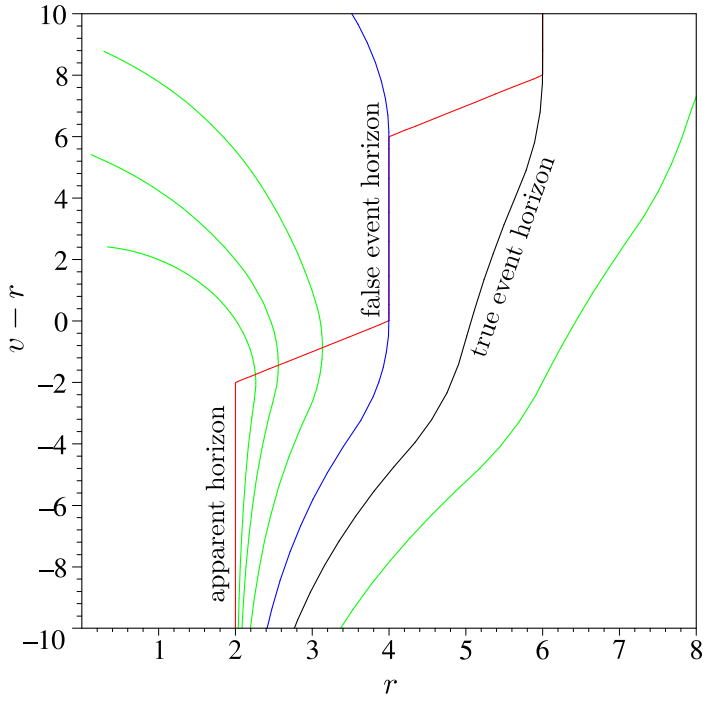

Figure 15: A variation on the scenario presented in Figure 14 with a second period of dust irradiation. If we were unaware of the second change in the apparent horizon — perhaps because we are given an incomplete metric from a numeric simulation — we would incorrectly identify the blue ray as the event horizon, while the true one is the black curve.

Again, we define the r coordinate via the area of the 2-sphere that it labels: $r^2 = \text{area}/4\pi$. But now, we must allow for the possible time dependence of the h metric function. Now, stacking these 3-geometries together in the most general way possible, we obtain:

$$ds^2 = -\bar{f}\, d\bar{t}^2 + \bar{h}\, dr^2 + r^2\, d\Omega^2 + d\bar{t}\,(A_r\, dr + A_\theta\, d\theta + A_\phi\, d\phi). \tag{136}$$

Before, we argued that the time reversal symmetry of the static case forced the **A** metric functions to be zero. In the dynamical case we cannot appeal to the same logic, so we need a different way to get rid of the them. Let's deal with the angular directions first. If we demand that our line element be invariant under rotations then the f and A_r metric functions ought to be independent of θ and ϕ. Now, a general rotation can be described by

$$\theta \to \tilde{\theta} = \tilde{\theta}(\theta, \phi), \quad \phi \to \tilde{\phi} = \tilde{\phi}(\theta, \phi) \tag{137}$$

The behaviour of A_θ and A_ϕ under this transformation is

$$A_{\tilde{\theta}} = \frac{\partial\theta}{\partial\tilde{\theta}} A_\theta + \frac{\partial\phi}{\partial\tilde{\theta}} A_\phi, \quad A_{\tilde{\phi}} = \frac{\partial\theta}{\partial\tilde{\phi}} A_\theta + \frac{\partial\phi}{\partial\tilde{\phi}} A_\phi \tag{138}$$

But invariance under rotations means that $A_{\tilde{\theta}} = A_\theta$ and $A_{\tilde{\phi}} = A_\phi$. Since this must hold for arbitrary rotations, the only solution is $A_\theta = A_\phi = 0$.

So our metric can be written as

$$ds^2 = -\bar{f}(\bar{t}, r)\, d\bar{t}^2 + \bar{h}(\bar{t}, r)\, dr^2 + r^2\, d\Omega^2 + A_r(\bar{t}, r)\, d\bar{t}\, dr. \tag{139}$$

But now we can transform

$$\bar{t} \to t = t(\bar{t}, r), \quad \bar{t} = \bar{t}(t, r). \tag{140}$$

Under this transformation, the metric becomes

$$ds^2 = -f(t,r)\,dt^2 + h(t,r)\,dr^2 + r^2\,d\Omega^2 + g(t,r)\,dt\,dr. \tag{141}$$

In particular,

$$g(t,r) = A_r(\bar{t},r)\frac{\partial \bar{t}}{\partial t} - 2\bar{f}(\bar{t},r)\frac{\partial \bar{t}}{\partial t}\frac{\partial \bar{t}}{\partial r}. \tag{142}$$

If we set $g = 0$, we get a first-order PDE for $\bar{t}(t,r)$:

$$\frac{\partial \bar{t}}{\partial r} = \frac{A_r(\bar{t},r)}{2\bar{f}(\bar{t},r)}. \tag{143}$$

Such a PDE can always be solved, even if only numerically, so we can always find a coordinate system in which $g(t,r) = 0$. Hence, the general time-dependent spherically symmetric line-element is

$$ds^2 = -f(t,r)\,dt^2 + h(t,r)\,dr^2 + r^2\,d\Omega^2. \tag{144}$$

Now, putting this *ansatz* into the vacuum Einstein equations $G^{\alpha}{}_{\beta} = 0$, we find that

$$G^{r}{}_{t} = 0 \quad \Rightarrow \quad \frac{\partial h}{\partial t} = 0; \tag{145}$$

i.e., h is a function of r only. Putting this into $G^{t}{}_{t} = 0$ yields an ODE for h with solution

$$h(r) = \left(1 - \frac{C}{r}\right)^{-1}, \tag{146}$$

where C is an arbitrary constant. The rest of the Einstein equations are satisfied if

$$f(t,r) = \left(1 - \frac{C}{r}\right) p^2(t), \tag{147}$$

where $p(t)$ is an arbitrary function of time. The time transformation $dt \to dt/p(t)$ then puts the metric into the final form

$$ds^2 = -\left(1 - \frac{C}{r}\right)\,dt^2 + \left(1 - \frac{C}{r}\right)^{-1}\,dr^2 + r^2\,d\Omega^2. \tag{148}$$

But this is precisely the Schwarzschild metric! We have discovered the Birkhoff theorem:

> *The only spherically symmetric solutions of the vacuum Einstein field equations are identical to the Schwarzschild metric up to coordinate transformations.*

This a very simple but very profound result. It says the no matter what kind of undulation that a spherical mass distribution undergoes, the metric outside of it is entirely static. Repeating arguments involving the motion of test particles, we can deduce that C is just twice the mass of the distribution. Therefore, just as in Newtonian mechanics the vacuum gravitational field around a spherical mass is solely dependent on its mass, and nothing else. It is curious that with all the complexities of the field equations of relativity that we recover this fundamental result.

2.3 Oppenheimer-Snyder collapse

We can now use the Birkhoff theorem to study the gravitational collapse of a ball of homogeneous dust. This problem was first considered by Oppenheimer and Snyder in 1939, hence the title of this section. Because of the Birkhoff theorem, the metric outside of the dust will be the Schwarzschild solution:

$$ds^2_{\text{out}} = -f\,dt^2 + f^{-1}\,dr^2 + r^2\,d\Omega^2. \tag{149}$$

Inside, we demand that according to observers comoving with out ball of dust, the spatial metric should be isotropic and homogeneous. This should ring a bell — it is the same requirement placed on Friedmann-Lemaître-Robertson-Walker (FLRW) cosmological models. This implies that we can take the metric inside the matter as

$$ds^2_{\text{in}} = -d\tau^2 + a^2(\tau)[d\chi^2 + S_k^2(\chi)\,d\Omega^2], \tag{150}$$

where

$$S_k(\chi) = \begin{cases} \sin\chi, & k = +1, \\ \chi, & k = 0, \\ \sinh\chi, & k = -1. \end{cases} \tag{151}$$

The stress energy sourcing the interior is that of dust:

$$T_{\alpha\beta} = \frac{1}{8\pi} u_\alpha u_\beta, \quad u_\alpha = -\partial_\alpha \tau. \tag{152}$$

The Friedmann equation governing the scale factor is found from the Einstein equations:

$$\left(\frac{da}{d\tau}\right)^2 + k = \frac{8}{3}\pi\rho a^2, \tag{153}$$

while the Bianchi identities yield

$$\rho a^3 = \text{constant}. \tag{154}$$

Our task is to now join these two solutions up at the boundary of the dust ball, which we call Σ.

The situation is very similar to one often encountered in other area of physics where we are interested in the solution of second order differential equations that change discontinuously across a boundary. Two examples include the scattering of wavefunctions off square barriers in one-dimensional quantum mechanics, and the solution of electromagnetic wave equations around the surface of a dielectric layer. In either case, the junction conditions are that the solution and its first derivative match across the boundary.[22] Since in our situation the second order differential equations are the Einstein equations and their solution is the metric, it makes sense to demand that $g_{\alpha\beta}$ and its derivatives are continuous across Σ.

[22] Actually, there is an important exception to the continuity of first derivatives in the electrostatic case; namely, that of a surface charge distribution. In that situation, the first derivative of the electric field is discontinuous across the boundary. It turns out that the same type of behaviour is admitted in the Einstein equations, where jumps in metric derivatives are associated with singular surface mass distributions. While this is extremely important for braneworld models, we won't consider such scenarios here.

But what does continuity of the metric mean? Clearly, the metric evaluated on the boundary should be the same if viewed from inside or outside the ball. In the exterior, we can identify Σ as

$$t = t(\tau), \quad r = r(\tau). \tag{155}$$

It should be obvious that these equation define a 3-dimensional timelike hypersurface, and "the metric evaluated at the boundary" is the induced metric of this hypersurface:

$$ds^2_\Sigma = -\left[f\left(\frac{dt}{d\tau}\right)^2 - \frac{1}{f}\left(\frac{dr}{d\tau}\right)^2\right] d\tau^2 + r^2(\tau)\, d\Omega^2. \tag{156}$$

Now, as viewed from the interior the boundary should be identified with by the trajectory of the dust particles on the edge of the cloud. Since these travel on curves with $\chi =$ constant, we can identify Σ by $\chi = \chi_0$:

$$ds^2_\Sigma = -d\tau^2 + a^2(\tau) S_k^2(\chi_0)\, d\Omega^2. \tag{157}$$

Comparing the two expressions for the metric on Σ, we find

$$1 = f\left(\frac{dt}{d\tau}\right)^2 - \frac{1}{f}\left(\frac{dr}{d\tau}\right)^2, \quad r(\tau) = a(\tau) S_k(\chi_0). \tag{158}$$

At this stage, we do not know the value of k, χ_0, or the solutions for $a(\tau)$ or $t(\tau)$. So we clearly have to do more to predict the behaviour of the system.

So the next task is to match the "derivative" of the metric across the boundary. To do this, lets construct a special coordinate system around Σ. We label $y^a = (t, \theta, \phi)$ and define a three dimensional tensor ${}^{(0)}h_{ab}$ by

$$ds^2_\Sigma = {}^{(0)}h_{ab} dy^a dy^b = -d\tau^2 + r^2(\tau)\, d\Omega^2. \tag{159}$$

We can then construct 4-dimensional coordinates near Σ by extending the 3-dimensional (t, θ, ϕ) coordinates orthogonally off of the boundary:

$$ds^2 = d\ell^2 + h_{ab} dy^a dy^b. \tag{160}$$

Note that we extend these coordinates into both the interior and exterior of the dust ball. In this system, which is called Gaussian-normal, the $\ell = 0$ surface is our boundary Σ and $h_{ab}|_{\ell=0} = {}^{(0)}h_{ab}$. Now, the derivatives of this metric parallel to Σ are obviously continuous because h_{ab} is well behaved. So, the only non-trivial requirement that we place on our metric is that the normal derivative across Σ is continuous:

$$\lim_{\ell \to 0^+} \partial_\ell g_{\alpha\beta} = \lim_{\ell \to 0^-} \partial_\ell g_{\alpha\beta}. \tag{161}$$

We immediately run into difficulties if we try to enforce this condition directly on either side of Σ because we don't have either spacetime metric written in Gaussian-normal coordinates. So, we need a coordinate invariant statement of our boundary condition. Notice that in the Gaussian normal coordinates we have that the unit normal to Σ is

$$n_\alpha = \partial_\alpha \ell, \quad n^\alpha = \partial_\ell, \quad n \cdot n = 1. \tag{162}$$

Then, we have

$$\nabla_\alpha n_\beta = -n_\gamma \Gamma^\gamma_{\alpha\beta} = -\tfrac{1}{2} n^\gamma (\partial_\beta g_{\alpha\gamma} + \partial_\alpha g_{\beta\gamma} - \partial_\gamma g_{\alpha\beta}) = \tfrac{1}{2} \partial_\ell g_{\alpha\beta}. \tag{163}$$

So we see that $\nabla_\alpha n_\beta$ reduces to the normal derivative of the metric across Σ in Gaussian-normal coordinates. In order to enforce our junction conditions, we should in some way make sure that $\nabla_\alpha n_\beta$ is continuous as viewed from either side of Σ.[23] But we can't quite do that directly, because $\nabla_\alpha n_\beta$ is a tensor whose components are surely different in different coordinate systems. Because we *are* using different coordinates inside and outside the ball, this can pose a problem in testing the continuity of $\nabla_\alpha n_\beta$.

The answer is to make sure that we compare scalars formed from $\nabla_\alpha n_\beta$ evaluated in the interior and exterior, as opposed to the individual tensor components. One such scalar can be composed with the 4-velocity of the dust particles defining the boundary Σ:

$$u^\alpha = \frac{dx^\alpha}{d\tau}, \quad u \cdot n = 0. \tag{164}$$

Since these trajectories are physical quantities they must be the same as viewed from the exterior and interior, although they will be written in terms of different coordinates. Then, the boundary conditions demand that

$$u^\alpha u^\beta \nabla_\alpha n_\beta = -n_\beta u^\alpha \nabla_\alpha u^\beta \tag{165}$$

is continuous across Σ. But in the interior $u_\alpha = -\partial_\alpha \tau$ is tangent to comoving geodesics, which implies that $u^\alpha u^\beta \nabla_\alpha n_\beta = 0$ on both sides of the boundary. In the exterior, the 4-velocity is

$$u^\alpha = \frac{dt}{d\tau}\frac{\partial}{\partial t} + \frac{dr}{d\tau}\frac{\partial}{\partial r}. \tag{166}$$

The lefthand equation in (158) guarantees that this vector is normalized $u \cdot u = -1$. Hence, the normal vector can be easily confirmed to be:

$$n_\alpha = -\frac{dr}{d\tau}dt + \frac{dt}{d\tau}dr, \quad n \cdot n = 1, \quad u \cdot n = 0. \tag{167}$$

We can then straightforwardly calculate that

$$u^\alpha \nabla_\alpha u^\beta = \mu n^\beta, \quad n_\beta u^\alpha \nabla_\alpha u^\beta = \mu, \tag{168}$$

where μ is a scalar. Our junction condition demands $n_\beta u^\alpha \nabla_\alpha u^\beta = 0$, hence $\mu = 0$ and u^α satisfies the affinely-parameterized geodesic equation. By now we have a lot of experience in working with this equation, so we just write down the solution:

$$\frac{dt}{d\tau} = \frac{E}{f}, \quad \frac{dr}{d\tau} = \pm\sqrt{E^2 - f}, \tag{169}$$

where E is the arbitrary energy parameter. Hence we now know that as viewed from the exterior, the boundary of the dust ball follows a freely falling trajectory.

Another scalar that must be continuous across Σ is $\nabla_\alpha n^\alpha$. Evaluating this on the boundary as seen from the interior:

$$n^\alpha = a^{-1}(\tau)\partial_\chi, \quad \nabla_\alpha n^\alpha = 2\frac{1}{a(\tau)}\frac{d}{d\chi}\ln S_k(\chi)\bigg|_{\chi=\chi_0}. \tag{170}$$

[23] We are going to some lengths to avoid introducing the notion of the extrinsic curvature of Σ in our treatment of the junction conditions because we simply haven't developed that formalism. However, the proper way to do things is to demand that the extrinsic curvature 3-tensor K_{ab} of the boundary is continuous. This quantity is simply related to $\nabla_\alpha n_\beta$.

In the exterior, we have

$$\nabla_\alpha n^\alpha = \frac{2E}{r(\tau)}, \tag{171}$$

where we have made use of the solution (169) for $dx^\alpha/d\tau$ furnished by the geodesic equation. Setting the two expressions for $\nabla_\alpha n^\alpha$ equal to each other and using the righthand equation in (158), we get

$$E = S_k'(\chi_0). \tag{172}$$

Then (158) and (169) together give

$$S_k^2 \left(\frac{da}{d\tau}\right)^2 = {S_k'}^2 - 1 + \frac{2M}{S_k a}. \tag{173}$$

Putting this into the Friedmann equation (153), we get

$$\tfrac{1}{2} S_k a({S_k'}^2 + kS_k^2 - 1) + M = \tfrac{4}{3}\pi S_k^3 a^3 \rho. \tag{174}$$

Note that for all k, we have ${S_k'}^2 + kS_k^2 - 1 = 0$. Hence we have

$$M = \tfrac{4}{3}\pi r^3(\tau)\rho(\tau). \tag{175}$$

This result is rather pleasing intuitively: the constant mass of the object in the exterior Schwarzschild geometry is precisely the product of the spatial volume of the dust ball (as measured by the comoving observers) and its density at any given time.

To sum up, we see that the dynamics of our spherical ball of dust is essentially determined from two constants: M and E. The former is that total mass of the dust and the parameter appearing in the exterior Schwarzschild solution. The latter is a measure of the kinetic energy of the ball and fixes the trajectory of the boundary via the integration of equations (169). From our previous discussion of geodesics we know that if $E < 1$ the boundary can never expand to or collapse from infinite size; i.e., the ball is gravitationally bound. If $E \geq 1$, the ball will indeed start up or end up with infinite radius, so these situations are somewhat unphysical even if mathematically allowed. Also, the relationship $E = S_k'(\chi_0)$ indirectly fixes k, since if $k = 1$ then $S_k' \in (0, 1)$, if $k = 0$ then $S_k' = 1$, and if $k = -1$ then $S_k' \in (1, \infty)$. The same relationship gives χ_0, and hence the position of the boundary according to observers comoving with the hole. Finally, the density of the dust follows directly from $M = \frac{4}{3}\pi r^3(\tau)\rho(\tau)$. Notice that the density of the ball becomes infinite as $r(\tau) \to 0$, indicating the formation of a black hole singularity as the ball collapses to zero size.

2.4 Penrose-Carter diagrams of gravitational collapse

It is interesting to note that in our search for dynamical dust ball solutions, we did not find any static cases. That is, there are no configurations of matter interacting purely via gravity that are static in general relativity. In the context of stars, this means that extra forces from nuclear furnaces are required to support the body against collapse, while in the context of cosmology this implies the expansion of the universe. The exact analogy between the dynamics of FLRW cosmologies and spherical matter distributions also implies "big bangs" and "big crunches" for our dust balls. For example, in the $k = 1$ case, the solution of the Friedmann equation (153) says that our ball starts with zero size, expands to some maximum radius a_m and then recollapses again. This all

takes place with finite time, so we have a purely Schwarzschild solution before and after the lifetime of the dust ball. The Friedmann equation gives the maximum radius of the ball in terms of the minimum in its density when we set $da/d\tau = 0$:

$$a_m^2 = \frac{3}{8\pi}\frac{1}{\rho_m}. \tag{176}$$

Putting this into (175) and using $r = a\sin\chi_0 = a\sqrt{1-E^2}$, we get the maximum radius in Schwarzschild coordinates:

$$r_m = \frac{2M}{\sin^2\chi_0} = \frac{2M}{1-E^2}. \tag{177}$$

Since $E < 1$ for $k = +1$ we have $r_m > 2M$; i.e., the turning point of the collapse occurs when the boundary is in Region I of the Schwarzschild geometry. Of course this is the way it must be, the boundary follows a timelike trajectory and it is impossible for such a trajectory to have a turning point in Regions II or III.

We can construct a Penrose-Carter diagram of the $k = +1$ dust collapse as follows: The surface Σ is identified as a radial null geodesic travelling from the white hole to black hole singularities. This divides the standard Penrose-Carter diagram of Schwarzschild in two. The half directly extending out to $\mathcal{I}^+$ and $\mathcal{I}^-$ is left as it is, representing the fact that the exterior of the dust is just the Schwarzschild solution. Now, inside the ball the $\chi = 0$ curve is the center of the geometry and is clearly a timelike surface, as are all the $\chi =$ constant curves in FLRW models. We can represent this part of the manifold as a straight vertical line which intersects the ball's boundary at the points where it touches $r = 0$; i.e., at the "big bang" and "big crunch." The result is in Figure 16. The blue region is the interior of the dust ball. We have drawn two interesting null geodesics on the diagram to illustrate how we are to interpret the timelike boundary of the manifold $\chi = 0$. The spatial geometry inside the ball is that of a 3-sphere, and $\chi = 0$ is like one of the poles. Now, on an ordinary sphere, when an object approached and crosses the north pole, the have θ decreasing to zero and then increasing again. If such a trajectory is drawn in the (t, θ) plane, the particle trajectory will be seen to be reflected in the boundary at $\theta = 0$. The same will be true in our Penrose-Carter diagram: the paths of particles and light beams are just reflected at $\chi = 0$. Hence, both the red and blue light beams shown in Figure 16 "bounce" off the $\chi = 0$ line. Interestingly, the fate of the two beams could not be more different. The red beam starts from past null infinity and hits the center of the dust ball before the blue beam and then escapes off to future null infinity. On the other hand, the blue beam ends up at the $r = 0$ singularity. The former ray corresponds to a light ray passing through the ball when it is least dense an incapable of gravitationally trapping it. The blue beam enters the cloud when it is more dense, and hence become trapped and ultimately ends up in the singularity.

Upon reflection on Figure 16, we realize that we still do not have a satisfactory model of the gravitational collapse of something like a star. The $k = +1$ Oppenheimer-Snyder solution describes an object that initially expands and then contracts, but a more realistic situation involves an initially static ball that — for whatever reason — collapses down to a black hole at some point in its lifetime. It is actually easy to modify our scenario to describe this phenomena, all we have to do is match the collapsing phase of the $k = +1$ Oppenheimer-Snyder solution with the metric around a static ball of matter at some time $t = t_0$, which signifies the start of the collapse. Physically, this time could represent the moment that a star runs out of nuclear fuel needed to provide the force counteracting the attraction of gravity. We will not go into the details of the

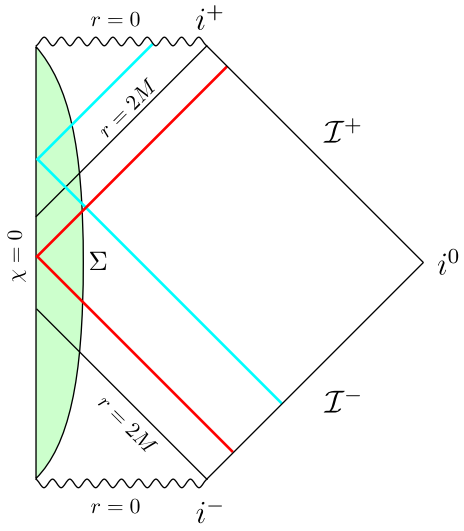

Figure 16: The Penrose-Carter diagram of the dynamics of a $k = +1$ dust ball in the Oppenheimer-Snyder formalism. The light blue region is the interior of the dust ball and the red and blue lines are representative light rays.

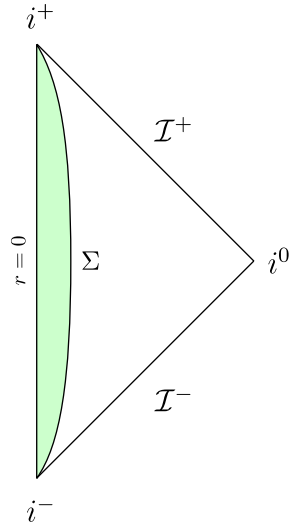

Figure 17: The Penrose-Carter diagram of a static star

static solution, for it is just the Schwarzschild solution joined with the matter metric at some $r = r_m > 2M$. For a static star there is no curvature singularity; since if there were, the matter near $r = 0$ could not actually be stationary, it would be inside the event horizon and would have to fall into the singularity. So what does the Penrose-Carter diagram of static star look like? This is given by Figure 17. The boundary of the star is a simple timelike curve and it center at $r = 0$ is a vertical line. The diagram is very similar to that of Minkowski space in Figure 7, except it is cut in half due to spherical coordinates. This is because the causal structure of the two situations is identical; there are no event horizons, singularities, etc.

Now, what does the Penrose-Carter diagram of the gravitational collapse of a spher-

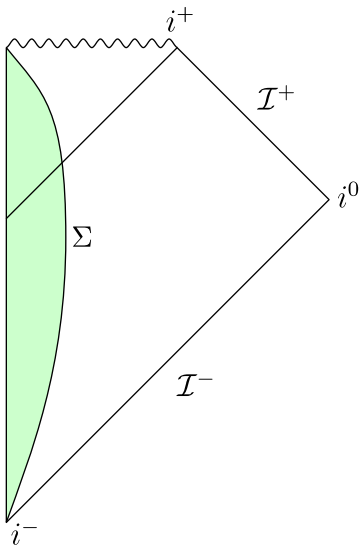

Figure 18: The Penrose-Carter diagram of the gravitational collapse of a spherical star

ical star into a black hole look like? It should be obvious that it is an amalgamation of Figures 16 and 17. This is shown in Figure 18. There are two comments to be made: First, although we have been considering a specific matter model up until this point, we expect this type of diagram to hold for any type of gravitational collapse. This is because the causal structure of the manifold will not care about the type of matter in the star; rather the only thing of importance is the paths of null geodesics. The only thing that may change is the precise shape of the Σ boundary. Second, when this diagram is compared with the ordinary Penrose-Carter diagram of Schwarzschild in Figure 5, we notice that Regions III and IV are absent. So there is no white hole in this diagram, nor a second asymptotically flat region. Recall that the existence of the white hole depended crucially on the existence of the spacelike singularity of Schwarzschild for all time, since it actually seemed to occur *before* $t = -\infty$. In the case of realistic collapse, the singularity only exists for a semi-infinite amount of time hence there is no white hole. Also, in the case of collapse the $r = 0$ surface is initially timelike and becomes spacelike as the singularity is formed. Since $r = 0$ is the boundary of our manifold, this forces us to cut off the maximally extended manifold shown in Figure 5 to the left of some vertical line. Hence, Region IV is effectively excised from the gravitational collapse manifold. Indeed, the amputation of Region IV is apparent even in Figure 16, because the expanding and recollapsing dust ball also involves a timelike boundary at $\chi = 0$.

Exercises

1. Find a coordinate transformation $r = r(\rho)$ that puts the Schwarzschild metric in the isotropic form

$$ds^2 = -H\,dt^2 + G\,(dx^2 + dy^2 + dz^2),$$

where $H = H(\rho)$, $G = G(\rho)$, and $\rho = \sqrt{x^2 + y^2 + z^2}$. What are the explicit functional forms of H and G? Is your transformation valid for all r?

2. Suppose that $u^\alpha = dx^\alpha/d\lambda$ is tangent to some geodesic curve γ. Under these circumstances, the parameter λ is said to be affine if the covariant acceleration of u^α is zero: $u^\alpha \nabla_\alpha u^\beta = 0$; for example, the proper time τ is an affine parameter along timelike geodesics. In what follows, assume that λ is not necessarily affine.

   (a) Use variational methods to show that u^α satisfies

$$u^\alpha \nabla_\alpha u^\beta = \kappa u^\beta.$$

   What is κ in terms of λ and the proper time parameter τ?

   (b) Show that $u^\alpha \nabla_\alpha u^\beta = 0$ implies that the length of u^α is conserved along γ; i.e., if λ is an affine parameter we have $d(u^\alpha u_\alpha)/d\lambda = 0$.

   (c) Verify the result in (a) for κ by applying a parameter transformation $\lambda = \lambda(\tau)$ to the 4-velocity $v^\alpha = dx^\alpha/d\tau$ in the affine-parameterized geodesic equation $v^\alpha \nabla_\alpha v^\beta = 0$.

   (d) Now suppose u^α satisfies

$$u^\alpha \nabla_\alpha u^\beta = \kappa u^\beta,$$

   with $\kappa \neq 0$. Under what conditions is the length of u^α conserved?

   (e) Finally, consider the situation where γ is not a geodesic but is timelike; i.e., the particle under consideration is massive and subject to some external acceleration $a^\alpha = u^\beta \nabla_\beta u^\alpha$. In this case, an affine parameter is defined as one for which the length of the 4-velocity is conserved. What does this imply for the acceleration vector a^α?

3. (a) Show that the vectors in equation (16) satisfy Killing's equation in general static and spherically symmetric spacetimes (7).

   (b) We define the commutator between vectors as

$$[u, v]^\alpha = v^\beta \nabla_\beta u^\alpha - u^\beta \nabla_\beta v^\alpha.$$

   Show that this is equivalent to

$$[u, v]^\alpha = v^\beta \partial_\beta u^\alpha - u^\beta \partial_\beta v^\alpha.$$

   (c) Calculate all possible commutators between $\xi^\alpha_{(1)}$, $\xi^\alpha_{(2)}$, and $\xi^\alpha_{(\phi)}$.

   (d) Now, relabel $\xi^\alpha_{(\phi)}$ as $\xi^\alpha_{(3)}$. Hence show that the triad of Killing vectors obeys:

$$[\xi_{(i)}, \xi_{(j)}]^\alpha = \epsilon_{ijk} \xi^\alpha_{(k)},$$

   where $i, j, k = 1, 2, 3$; ϵ_{ijk} is the standard permutation symbol; and there is no summation on the Latin indices.[24]

[24] This leads to a better definition of spherical symmetry; i.e., a spherically symmetric spacetime is one with a triad of Killing vectors tangent to 2-spheres that obeys the above relation. In group theory language such an expression defines an *algebra*; in particular, here we see the algebra of SO(3).

4. Show that a photon can have a circular orbit around the central object in the Schwarzschild geometry and determine its radius. Is the orbit stable?

5. Consider a non-planar electromagnetic wave in special relativity. We assume that such a wave can be described by a vector potential

$$A^\alpha = c^\alpha e^{i\phi},$$

where c^α is a constant vector and the phase ϕ is a general spacetime scalar. This will be a solution of the vacuum Maxwell's equations:

$$\partial_\alpha F^{\alpha\beta} = 0, \quad F_{\alpha\beta} = \partial_\alpha A_\beta - \partial_\beta A_\alpha.$$

   (a) Specialize to the Lorentz gauge where $\partial_\alpha A^\alpha = 0$. Hence, show that the Maxwell equations reduce to

$$\partial^\alpha \partial_\alpha A^\beta = 0.$$

   (b) Now define the wavevector as $k_\alpha = \partial_\alpha \phi$ and show that

$$\partial_\alpha k^\alpha = 0, \quad k_\alpha k^\alpha = 0.$$

   (c) Finally, apply ∂_β to $k_\alpha k^\alpha = 0$ in order to obtain

$$k^\alpha \partial_\alpha k^\beta = 0.$$

   Hence, in special relativity the wavevector of electromagnetic radiation is the same as the affinely-parameterized tangent vector to a null geodesic.

6. We have been working in geometric units where $G = c = 1$. If we instead work in standard units, the Schwarzschild solution is

$$ds^2 = -f\, d(ct) + \frac{1}{f}\, dr^2 + r^2\, d\Omega^2, \quad f = 1 - \frac{C}{r}.$$

   (a) By demanding that Newton's law is recovered at large r, determine the value of C in these coordinates.

   (b) Suppose that an observer falls through $\mathcal{H}$ in the Schwarzschild geometry. What is the maximum amount of time it will take for them to collide with the singularity, provided that the central object has the mass of

      i. the sun?

      ii. our galaxy?

7. The 5-dimensional generalization of the Schwarzschild solution is

$$ds^2 = -f\, dt^2 + \frac{1}{f}\, dr^2 + r^2\, d\Omega_3^2, \quad f = 1 - \frac{r_0^2}{r^2},$$

   where $d\Omega_3^2$ is the metric on a unit 3-sphere. Ignoring the angular directions, perform a maximal extension of this spacetime by finding suitable Kruskal coordinates.

8. Consider two conformally identical n-dimensional metrics. Show that in a certain coordinate system, the null geodesics of each have exactly the same form $x^\alpha = x^\alpha(\lambda)$.

9. Explicitly construct the Penrose-Carter diagram of Minkowski space shown in Figure 7.

10. Derive equations (95).

References

[1] C. W. Misner, K. S. Thorne, and J. A. Wheeler. *Gravitation*. Freeman, New York, 1970. Everything you ever wanted to know about everything, but with sometimes strange notation.

[2] Eric Poisson. *A Relativists Toolkit: The Mathematics of Black-Hole Mechanics*. Cambridge University Press, 2004. Introduction to many advanced topics in relativity, highly recommended.

[3] R. M. Wald. *General Relativity*. University of Chicago, Chicago, 1984. The standard text on modern relativity. Good treatment of singularity theorems, black hole evapouration, and related topics not covered in these notes.